

Material Solution to Reducing Wear and Erosion of Choke Valves and Separators in the Oil and Gas Industry

Tortor, J. Tom

*Department of Petroleum and Gas Engineering, Faculty of Engineering,
Nigeria Maritime University, Okerenkoko, P.M.B. 1005, Delta State, Nigeria*

Submitted: 03-11-2021

Revised: 25-05-2022

Accepted: 28-05-2022

ABSTRACT

In the oil and gas industry, engineers are constantly looking for material solutions on how best in improving the business of hydrocarbon exploration, production, refinery process and transportation. There is always a growing need to ensure assets integrity in compliance with existing regulation and greater environmental protection. Oil and gas facilities integrity and frequent equipment maintenance is a growing concern to many companies' management. As oil and gas production moves into extreme hard to reach challenging subsea offshore harsh environment, at the same time, the need for developing the finest material solutions to confront erosive-wear and corrosion, and other harsh environmental and operating conditions is increasing. There is always the need for meeting competing demands and making trade-offs between profit and investment.

Balancing these growing needs of profit and investment, assets/facilities integrity and solving the mirage of hydrocarbon production challenges require creative engineering solutions. Equipment reliability during design and using the most appropriate materials in manufacturing the oil and gas industry equipment that handles the complexity of production fluids require careful engineering material solutions that can improve efficiency and eventual resolution of complex problem such as wear and erosion in the oil and gas industry.

Keywords: Erosion, Wear, cavitation, separator, choke valve, model, Stellite Alloy, Oil & Gas Industry

I. INTRODUCTION

The concept of material solutions to reducing wear and erosion in the oil and gas industry postulated in this research is an integrated engineering approach to solving the challenges posed by erosive-wear in critical hydrocarbon productions equipment such as choke valves and separators. In evaluating the use of advanced composite materials to combating these

complex problems comes with a wide range of engineering challenges which includes the damage mechanism of these materials, structural composition, thermal stability, elastic properties, resistivity, design and manufacturing, and a host of others.

There are limited arrays of oil and gas industry accepted finite element simulations, empirical models, equations, and of course calculations, which allows for materials erosive-wear determination comprehensively, and accurately simulates the effects of these conditions on oil and gas structural equipment. In the oil and gas industry, the choice of material used solely depends on the purpose, the operating environment, and the operational in-service conditions in which such materials will be subjected are top priority in the design and manufacturing of such equipment. Degradation of material in production facilities cannot be completely circumvented (Haugen, 2011).

However, the application of appropriate materials solution such as advanced material selection in the design and manufacturing process, critical analysis of the fluid characteristics, flow rate, geometry of the flow regime, particles concentrations and impingement angle, proper material surface treatment and prevention, effective wear and erosion mitigation, full appraisal of the solid particle erosion mechanism and other corrosion-erosive wear reducing methods will definitely surmounts the menace of wear and erosion in the industry. Hence, this study seeks to provide a material solution that are efficient and cost effective to reducing wear and erosion in the oil and gas industry.

1.1 Contextual

Erosive wear is a very problematic issue facing infrastructures in the oil and gas industry. Wear in this context, can be defined as the damage to a critical oil and gas component due to interfacial interaction of fluid particles and the internal surface of

the equipment that causes unwanted material erasure from the mechanically interacting/or impingement surfaces; while erosion is the gradual surface degradation due to contact with contaminated reservoir fluid flowing in the oil and gas production facilities. These phenomena are extremely detrimental and malignant to the oil and gas production, transportation and storage infrastructures causing damage to such equipment as choke valves and separators just to mention a few, and economical/financial loss.

Choke valves and separators are commonly affected by wear and erosion caused by production fluid that are contaminated by sand and iron particles, and other corrosive impurities such as CO₂, H₂S etc., routinely flowing through and into this equipment. Due to the abrasive and corrosive nature of this contaminants, they tend to cause wear and erosion in these production equipment(s) by way of removing materials from the choke valve and separator as a result of the repeated fluid impartation on the internal surface of these equipment(s). These malignant problems are worsened by the fluid flow characteristics that exist in the system.

For example, the angle of impingement of the solid particles on the internal surface of the trim of choke valves can greatly influence the rate of erosive-wear of the materials at the point of impact (Knollenberg and Sontvedt, 1995). Also, the mechanical properties such as elastic properties (modulus of elasticity, fracture toughness, and yield strength) of the materials can greatly determine the level of erosion and wear degradation. The operating conditions are not left out. The influence of pressure, temperature, flowrate and all other in-service environment conditions accelerates the rate of material degradation in these components (Atapek, 2015).

1.2 Nature of the Challenge

Corrosive reservoir fluid (hydrocarbon) with suspended sand, and metal particles are constantly flowing through production facilities. The impartation of this fluid on the internal surface of these equipment causes wear and erosion to the materials thereby, reducing surface thickness and eventual failure of the equipment (Bitter, 1963). Eroded choke valve and separator can cause failure resulting to environmental degradation and financial loss in the oil and gas industry. Therefore, it is vital to know the phenomenon that governs wear and erosion and how a good material selection in the design and manufacturing process can eliminate wear and erosion of critical equipment in the oil and gas industry.

This research seeks to describe the prominent factors that influences wear and erosion, and examine the failure modes associated with separators and choke valves (as a case study), due to wear and erosion and critically review available literatures on the mechanism of solid particle erosion. Additionally, empirical model

and equations for erosive wear in separators and valves that can be used in the oil and gas industry to reduce wear and erosion damages are extensively discussed.

Ultimately, a comprehensive material solution using **Cambridge Engineering selector (CES)**, with greater precision and optimization of required information in selecting appropriate materials of the highest quality for designing this equipment has been put forward, and a comprehensive surface engineering methods including surface modification, surface treatment and surface coating are explained in detail.

Material interface functionalization's and coating deposition methods such as carburisation, chemical vapour deposition (CVD), nitration, transformation hardening, physical vapour deposition (PVD), and ion impartation are evaluated. Finally, knowledge gap and limitations that are possible regarding wear and erosion are specified. This work can be employed by multinational oil and gas companies as an in-depth review of wear and erosion problems and remedy in the oil and gas industry. Thus, this study will bridge the existing knowledge gap on ways of preventing wear and erosion related damage in oil and gas infrastructures.

II. LITERATURE REVIEW: HISTORY OF WEAR AND EROSION IN THE OIL AND GAS INDUSTRY

Material erosion in oil and gas is a wear process that affect the production equipment in the industry. To fully understand erosive wear problem in the oil and gas industry and be able to select a suitable advanced material that can reduce erosive wear, one need to understand and access holistically the erosion phenomena in detail and in context. The origin of erosive wear and its effects is as old as the oil and gas industry.

However, existing research works on the erosion and wear of metals in the oil and gas industry has strong focus on empirical, experimentation, and lately simulation on both the flow condition and the surface impartation procedures. The earliest works by Finnie (1958 and 1960) shows greater concerns expressed by various authors on material surface wear and erosion by torrent of suspended solid particles over the years and proposed models for micro substrate of ductile material as a direct result of micro cuttings (Finnie, 1958). However, due to the rate of under predictions of the magnitude of erosion from the particle surface impingement at greater angles (<90°) as shown in experimental data, he modified his models to take into consideration these weaknesses observed in the earlier model (Finnie, 1960).

Erosive wear of material as regard to loss of the material wall thickness depends on several

interconnected issues ranging from the targets bulk material structures and properties, macro and micro exposure circumstances, both the erodent's particles, chemical/physical characteristic, and the high temperature which is a function of the existing chemical surroundings of the target surface, which initiate the erosion or corrosion effect of the material (Alan 1997).

Different researchers, in a bid to critically examine and give a proper and more realistic definition of erosion wear of material have come up with various postulations. For example, Finnie, (1967) define erosive wear as 'the elimination of material from a hard surface through the actions of impingement by a fluid or solid particles. However, this descriptive definition specifically ignores progressions which could be able to correctly dubbed erosive wear.

In 1979, while addressing a conference on erosion, Tabor defines erosion further, in generally mechanical terms as, 'involving the repeated applications of stresses that are high and local which in several cases are applied in very limited time interval' (Tabor, 1979). However, this definition restriction of time fails to recognize the continue flow of fluid through production streams and the continue impingement of solid particles on the walls of the equipment during this time period.

A more realistic, thorough and comprehensive definition is that of the American society for Testing and materials (ASTM, 1993), which defines erosive wear as 'the progressive loss of novel materials from a solid surface which is due to mechanical interactions between the surface and a multicomponent fluid (e.g., hydrocarbon that contains abrasive, and adhesive sand particles), impingement liquids or solid flocculating fluids suspended particles in the flow stream'. This definition comprises all the three fundamental dissimilar type of wear due to erosion which includes:

- Erosive wear due to impingement by solid particles,
- Erosive wear due to liquid droplet impingement and
- Erosion due to liquid cavitation.

The 'mechanical interactions' contained in the above definition suggests as separating erosive wear due to corrosion which is the chemical interactions. However, one can conveniently argue that greater main stream of occurrences of erosion in the oil and gas industry is always in combinations with corrossions damages.

Concerted efforts expended to precisely calculate the actual quantity of wear that a component material will experience in any engineering oil and gas industry application as regard to erosive wear has been widely made. There are several reasons for the need to accurately measure erosive wear (Peter,1996). These reasons include: To obtain data for designing of new equipment, for effective material surface treatments,

effective research and developments of oil and gas equipment and, effective prevention and appropriate maintenance interval determinations.

Researchers over the years, have made considerable exertions directed in relation to elucidate the erosive wear mechanisms. These exhaustive researches are generally geared towards minimizing the problematic and undesirable erosive wear and corrosion related effects that are causing the loss of billions of dollars yearly in the oil and gas industry.

However, some researchers such as, (Meguid, *et al*, 1976) argued that, erosion can sometimes, have advantageous effects, citing 'short peening and peen forming processes' in some industry as an example. Nevertheless, one can argued that such processes with regards to erosive wear as it affects the oil and gas industry critical infrastructures such as choke valves and separators is invalid. Reason being that, the benefits of such process cannot be compared to the economic damage failure of any of this equipment due to erosion can cause including its adverse environmental impacts.

2.1 Materials Wear and Erosion

Material wear is mostly classified into three key groups in the oil and gas industry. These are: abrasive wear/adhesive, sliding wear, and erosive wear. Two solid exteriors relatively moving in opposite direction while in contacts causes the occurrence of abrasive wear. The controlling factors of the scratchy resistance of the materials is the 'size and volume' of hard phases in that material (Opris *et al*, 2007).

In case of wear due to sliding, three basic mechanisms are involved which are: fatigue of sub-surface, stresses caused by the contacts, and control of oxides. Resistances to material wear due to sliding is chiefly depended upon that material total stiffness and strength (Amateuet al, 1964).

However, the complex characteristics of material progressive degradation is known as the erosion wear (Reddy and Sundararajan 1986) and (Oka *et al* 2009). In this case, particles impartation and cavitation shockwave on surfaces result in wear due to erosion. The sudden collapse of gas bubbles in a flowing fluid at the surface of a material generates cavitation erosion, while solid particles impingement against a material surface leads to the occurrences of slurry and liquid entrain-particle erosion.

Therefore, a single property of materials is not reasonably sufficient to predicting a material erosional wear resistivity (Glaesser *et al*, 1994) and (Sydney 2013) as previously mentioned.

2.2 Material Erosion mechanisms

Heuristic methodology seems prospectively, continue to be the more suitable way of erosive wear

prediction given the existing complexity of flow conditions prevalent in the oil and gas industry. Reason been that there are huge mechanism/parameters seen to be influencing the proportion of erosive wear and these mechanisms are interconnected (David, 1980). For instance, the eroding substance impingement angles, particles geometry, spot of impingement, velocity of particles, particle size, shape etc., are seen not to be independent considering the fluid flow dynamics around the impingement spot.

In order to proffer a proper advanced material solutions in reducing erosion wear, one needs to critically examine and review the various erosive wear mechanism prevalent in the oil and gas industry. Presently, based on the verse array of available literatures on erosive wear reviewed, there seems to be only 'limited agreement' on views concerning which mechanisms are principal as regards to ductile or brittle erosive wear scenario in the oil and gas industry.

Erosion wear mechanisms that seem to have gained generality of recognition as proposed by different authors includes:

- Impingement angles of erodent particles
- Behaviour of erodent particle target surface materials properties
- Ductile materials surface erosion
- Brittle materials surface erosion

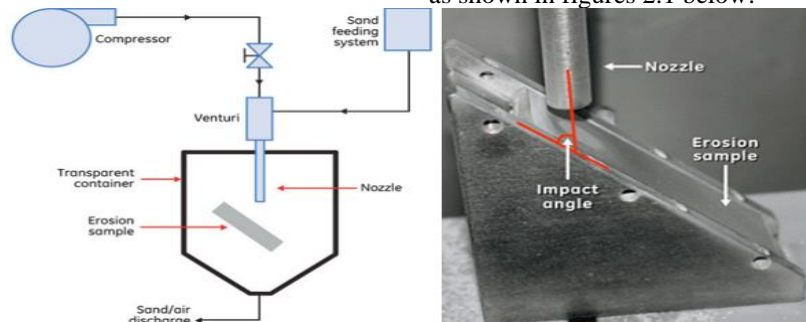


Figure 2.1: A Schematic diagram of the impingement angle test facility & assembly (Guruprasad *et al*,2012)

It is observed that in every known material for oil and gas industrial application, there consists critical angle of impingement in which there will be an occurrence of maximum erosive wear. The critical impingement angle for ductile material such as metallic alloys ranges from 15° – 30° , and brittle (inelastic) materials such as glasses and ceramics, the occurrence of the critical angle is about 90° (S. Kamran *et al*, 2011).

However, it is observed in most literature reviewed that, determination of the critical angle for erosive wear via experiment is practically impossible (Kamran *et al*, 2011). This is owing to the fact that there is no single

- Velocity of erodent particles
- The erosive wear particle sizes
- Shapes, flowrate and hardness of erodent particles
- Wear due to fatigue of the surface been eroded by more particle's repetitive impartation
- Temperatures and conditions of the fluids (gas or liquid), and environmental conditions prevalent,
- Etc.

The list is inexhaustive. However, some of the most critical erosive mechanisms highlighted above are discussed in detail in the following sub-sections of this study, so as to gain useful insight to the erosion wear problems in the industry.'

2.3 Broad Cases Review on Some of the Critical Parameters causing Erosion Wear Rate in the Oil and Gas Industry Generally Agreed by Previous Researchers.

2.3.1 The impingement angles of erodent particles

The impingement angle is defined as the angle stuck between the pathways the erodent particles follows and the targeted materials, and it is also called the impact or impingement angle (Oka *et al* 2005). This is also cited in the works of (Guru-Prasad *et al*, 2012), as shown in figures 2.1 below:

affinity for all materials to behave in the same conditions, the same way due to different material composition, limitation of time and equipment, and also, the erodent particles sizes and shapes which can greatly impair experimental results (Oka *et al*, 2009). More so, critical impingement angles vary in most materials with respect to the impact velocity of the particles (Oka *et al*, 2009).

Figure 2.2, illustrates ductile (metallic alloys) materials, and brittle (glass and ceramic) materials erosive wear behaviours under impact angles between the ranges of 0° – 90° respectively.

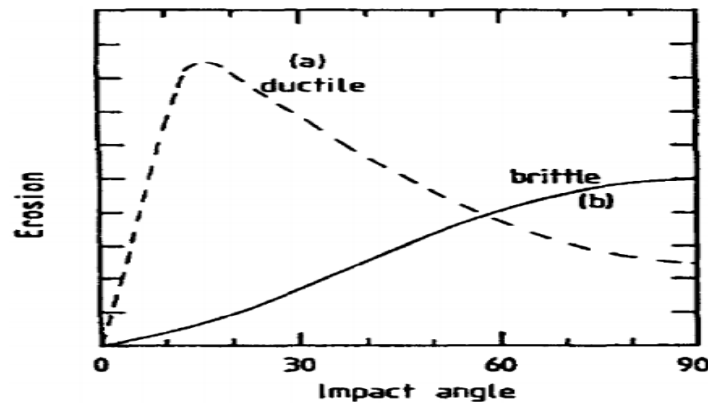


Figure 2.2: Showing a schematic diagram of the impingement angle influence on erosive wear rate both in ductile and brittle materials (K. Haugen et al, 1995).

2.3.2 Behaviour of erodent particle target surface materials properties

The erosive wear of a target surface material will be influenced significantly by the material mechanical property such as stiffness, fracture toughness and ductility. As we know, the stiffness of a material in most cases, is very important and known to be typical representation of the mechanical properties of that material (Sundararajan and Roy 1997). Material strengthening mechanism for example, solid solutions and cold works strengthening can immensely improve erosive wear resistance of single-phase metallic alloys. However, there could be some exception that additions of some element for example, solutes such as (Al, Zn, etc. added to Cu) will generally increase the strength of the materials but will not necessarily increase the erosive wear resistances (Ashby and Cebon, 1993). Studies on multi-phase metal such as carbon steel containing dissimilar carbon content has shown lower erosive wear resistance of the high carbon contents steel as reported by (McCabe, A. Sargent and Conrad, 1985:257-277p). Alloys with dispersion strengthening has often shown higher erosive wear rates than similar alloys that are without dispersions in their micro structures (Ashby and Cebon, 1993). However, it is worthy to note here that within metal material, there

continuously exist a minor disparity in the sensitivity of afore mentioned erosion degradation, severity predictive parameters. Thus, this has resulted to the overwhelming requirement of case-by-case investigation of erosive wear degradation difficult and strenuous.

2.3.3 Ductile Material Surface Erosion

Ductile material surface erosion mechanism is dependent upon “ductility – substrate materials plastic distortion/deformation capabilities” (Swanson, 2016). However, this proposition gains credibility is cited in the works of Finnie (1958; 1960 and 1972), and also cited in the works of (Mazdak Parsi et al., 2014). Other researchers as shown that particles surface impingement creates low craters in the form of platelets fragments (Levy et al, 1981), and that they are easily separable by successive particles impingement as illustrated in (figure 2.3) below. It is also shown that ‘detachment of the platelets formed at the material subsurface from the edge of the wear crater is due to the shear heating of the material surface, and localized work hardening (Swanson, 2016). The high erosive wear rate in the steady state situation as compared to the initial erosive wear rate is explained by the above mention platelet formation process (Parsi et al, 2014).

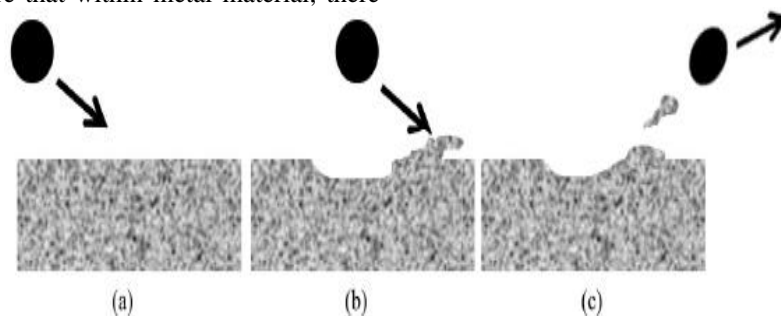


Figure 2.3: A Schematic diagram showing ductile material surface erosive wear procedure (a): before Impingement (b) Crater and pilling of material at one side of the crater, (c): Material separation from the surface (M. Parsi et al 2014).

2.3.4 Brittle material surface erosion

The brittle materials erosive wear is largely attributable to cracks formations and chippings because brittle materials fundamentally have no plastic distortion capabilities (Levy, 1995). At particles initial collision on the material surface, there is formation or propagation of radial cracks. Subsequent impact by

particles within the crater locality causes the further propagations of the cracks initially generated. This will fragment the material surface in the vicinity into several angular particles that will be removed by subsequently impacting particulates (Swanson 2016); (levy 1995); and (Parsi 2014). This above-described phenomenon is illustrated in (Figure 2.4) below:

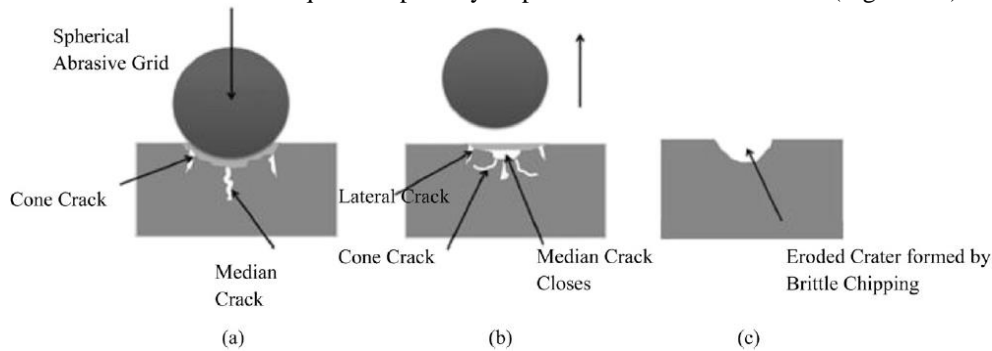


Figure 2.4: Showing Schematic diagram of the erosion mechanism of ductile material: (a) conical growth of cracks and median crack (b) closure of median and creation of lateral cracks, (c) eroded crater formed (Adopted from: Parsi et al, 2014).

2.3.5 Velocity of Erodent particles

Nearly all researchers from the literature reviewed agreed to the fact that the velocity of erodent particles is an utmost important parameter that is affecting erosive wear rate. The erosive wear rate of materials is defined as ‘a ratio of targeted material to the quantity of the erodent particles striking the surface (Sundararajan and Roy 1997: 339-359p). More researchers have proposed that erosive wear rate (ER) could be expressed as a function of velocity of impact, (V) in the following expression below (G. L Sheldon and A. Kanhere 1972:195-209p):

$$ER = E_0 V^p \text{-----(1)}$$

Were,

$ER = \text{Erosive wear rate}$

$E_0 = \text{Constant}$

$V = \text{Velocity}$

$p = \text{Velocity exponent}$

Several erosive wear experimental data on the velocity of impact on metal material in tilted impact condition by researchers collected shows that the average

exponential velocity (p) ranges between (2.4 – 2.55) (Hutchings,1979: 393p). Others suggested that the impact velocity can be as high as 5 for composites of polymer matrix and that parameters like sizes of the erodent particles, shapes, impingement angle, etc., could also affect or contribute to the velocity exponent as regard erosion (Sundararajan and Roy 1997: 339-359p).

Velocity exponent decrease with regards to decrease in the sizes of impact particles is also observed in some experimental results. However, some recent researchers of erosive wear have argued that, the velocity exponential is not a constant but depends on the eroded material stiffness which could varied with different materials composition and mechanical properties (Oka et al, 2005).

Generally, it is seen from experimental data’s that higher erodent velocity will lead to higher rate of erosion of material, and higher rate of erosion of material is as a result of higher particles impingement velocity. This is vividly illustrated in the (Figure 2.5) below:

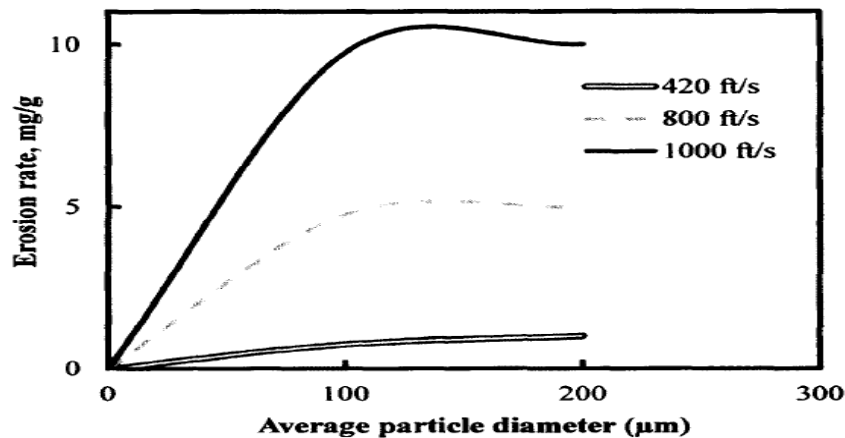


Figure 2.5: Schematic diagram for the varying erosion rate of steels with particles sizes at dissimilar impingement velocities (G. Sundararajan and M. Roy 1997).

2.3.6 The Erosive Wear Particle Sizes

Another significant erosive wear mechanism/property is the particle size which has great influence on the rate of material erosion. Earlier researchers have reported increase erosive wear rate with various particle size with no significant variation of rate of erosion, if the erodent particle size is greater than 50 – 100µm (Sheldon and Finnie, 1966). However, recent researchers such as (Desale *et al*, 2009), has examined particle size effect on the erosive wear rate of (aluminium alloy AA 6063), and found out

that increasing the particle size will certainly increase the erosive wear rate at a constant erodent (sand) concentration. Although the number of sand particles and impingement at a given time were observed been reduced. Also, the experiment was conducted using dissimilar sand (silica) sizes ranging from (37.5 to 655µm) with fluid velocity of (3m per second), (20wt% erodent sand concentration) and impingement angles of (30 and 90degrees). The results are shown illustrated in (figure 2.6).

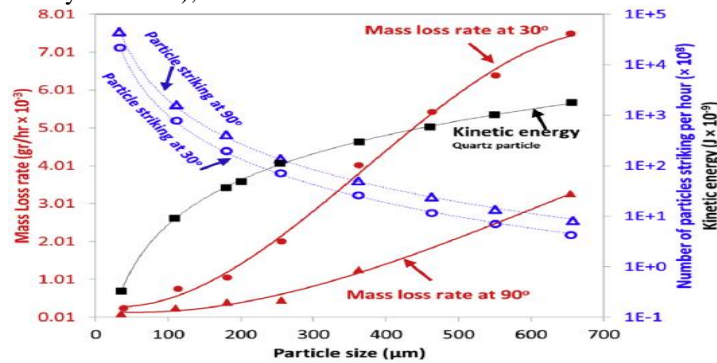


Figure 2.6: Sand (silica) particle effect on erosion wear rate of AA6063 Aluminium alloy as target material and number of impinging particles showing mass loss rate at 30° and 90° with different particle sizes (Desale *et al*, 2009)

Generally, finer erodent particles will have lesser erosive wear rate because of their lesser kinetic energy and lesser impingement load on material surfaces as a way of eroding the material (Ashby, and Jones, 2005). In addition, erosion of material is also affected by particle shapes, density, hardness, fluid viscosity and velocity as afore mention with a host of other properties. Even though a lot of suggestions has been made with regard to the particle size's effects, there seems to be no generally accepted explanation fitting for all application.

2.3.7 Shape, Flowrate and Hardness of Eroding Particles

Other parameters worthy of note is the shape, fluid flowrate and the hardness of the erodent particles. Angularly shaped solid particles tend to cause higher material erosion rates than sphere-shaped erodent particles on numerous metal materials. Some literature reviewed showed that there is a slight shift impact angle from 30° – 90° in the erosive wear tests on Cu alloys eroded with sphere-shaped erodent particles. Maximum erosion rates were recorded at impact angle of 90°. A reversed behaviour was witnessed when angular silicon carbide (SiC) erodent was used and a

ductile erosive wear damage was observed as can be seen in the (figure2.7) has being investigated by (Reddy and Sundararajan, 1986: 313-323p).

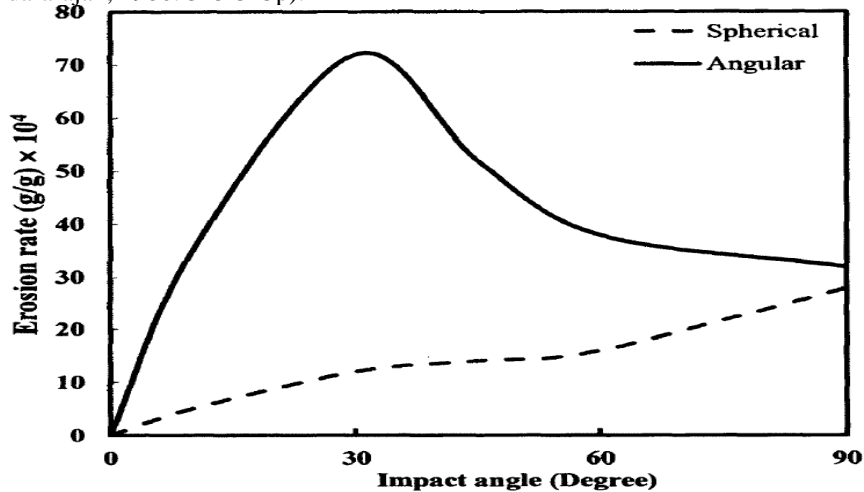


Figure 2.7: A schematic diagram showing the particles shape effect on the rate of erosion (Sundararajan and Roy 1997).

Flowrate of the erodent particles has also been investigated. Erosive wear rate of metal material is scarcely influenced by impact particles flowrate. This is due to the rebounding of particles on each other as they flow in high rate causing exponential trends of decrease of erosive wear rate (Sundararajan and Roy 1997: 339-359p).

Erodent particles hardness is also worthy of note. Researchers have observed that rate of erosion in stainless steel was observed completely independent of the hardness of eroding particles if the target material is at minimum twice lesser than the erosive wear particle (Levy 1995). Researchers have not found a general trend with regards to the effect of the “hardness erodent particles (Sundararajan and Roy 1997).

III. PREVIOUS EROSIWE WEAR RESEARCHMETHODOLOGIES

The qualitative case research methodology applied in the present research, is to critically discuss the complex erosion wear phenomena presently existing in the oil and gas industry, evaluate the critical challenges and relative materials solutions put forward by previous researchers in mitigating the problems with regard to erosion wear rate of surface materials for the design and manufacture of oil and gas engineering critical components.

Thereby, an overview of the methodology used by previous researchers in determination of the erosion rate in the oil and gas industry, the challenges, causes and effects are critically evaluated. This is imperative for the fact that, almost 40% of hydrocarbon reserves in the world contains some level of sour gas such as hydrogen sulphide (H₂S), carbon dioxide (CO₂) and of

course, other impurities such as solid particles that are detrimental to production and processing equipment, which cause erosion wear and other challenges in the industry (Total,2016). Generality of the cases studied agreed to the malignant solid particles impingement as the most prevalent cause of the erosion wear rate of material surface in most oil and gas components.

Solid particles and sour gases (naturally occurring long chain hydrocarbons containing organic sulphur compound) have damaging effects on surface equipment, for example, choke valves, pumps, separators, flowlines, and well tubing accessories. Therefore, this equipment must be made of special materials since these gases accompanied with sand-solid particles causes erosion wear and corrosion to production equipment.

1.3 Field Based Case Study: Erosion of Wear Resistant Materials: Erosion in Choke Valves in Oil and Gas Application

Haugen et al, (1995) conducted a research on the sand particle erosion wear resistant material and study the erosion wear behaviour of twenty-eight different oil and gas industry application materials such as tungsten carbide material, standard steels ceramics and coating materials which are the most used and/or considered as future materials in the industry .The focus of the study was to finding materials that can increase the longevity of processing equipment components such as choke valves in the industry, through design optimizations and erosion resistance materials.

The testing of the above mention materials was done considering the critical erosion parameters

already mention above such as various impact angles ranging from (7.5° – 90°), angular (sand) particles size up to 200 to 250µm, typically found in the North-sea oil fields, and velocities ranging from (18, 20, 40, 45, 200 and 220m/s) in that respective order. Carbon-steel grade was selected as the test reference material and as such was tested extensively with deferent parameters and the standard impact angle of 22.5° and 90° as the guide angle since the critical erosion rate occurs in between these angles in both brittle and ductile materials. The test procedure and comprehensive details can be found in (Haugen et al, 1995). A three-step modelling of the erosion wear process in choke valves was implemented to support the experimental results. The steps include:

- Modelling the hydrocarbon fluid flow behaviour in the production system
- The solid particles behaviour within the hydrocarbon fluid flow and
- Specific modelling of the erosion wear attack by the particle’s impingement in the internal components of the choke valves such as the valve trim (Haugen et al, 1995).

The general correlation of the erosion wear rate empirically established and also cited in the works of Table 1: Shows the weight loss (mg per kg sand) as function of particles impact velocity and impingement angles (Haugen et al, 1995).

| V _p | 45–50 m s ⁻¹ | | 200–220 m s ⁻¹ | |
|--------------------------------------|-------------------------|-------|---------------------------|-------|
| | 90° | 22.5° | 90° | 22.5° |
| C-steel | 14 | 23 | 1085 | 1700 |
| 316-steel | 16 | 20 | 1770 | 1845 |
| Duplex | 13 | 23 | 1400 | 1825 |
| SMO | 12 | 20 | 2170 | 1690 |
| Stellite | 17 | 13 | 1870 | 1030 |
| Boronized Stellite | 1.7 | 1.7 | 860 | 265 |
| Electrochemical nickel Ni-250 | 15 | 27 | 1070 | 1930 |
| Electrochemical nickel Ni-500 | 17 | 22 | 1460 | 1460 |
| Hot sprayed WC-60%Ni | 27 | 13 | 4670 | 1145 |
| Hot sprayed WC-40%Ni | 32 | 17 | 4070 | 1470 |
| Detonation gun WC, thin layer | 108 | 33 | 13000 | 2700 |
| Cobalt based coating | 70 | 50 | 7100 | 4200 |
| Degun WC, 0.25 | 16 | 4 | 860 | 265 |
| WC, DC 05 | 0.7 | 0.58 | 22 | 11 |
| WC, CS 10 | 1.6 | 1.0 | 45 | 17 |
| WC, CR 37 | 1.2 | 0.83 | 50 | 17 |
| 95% Al ₂ O ₃ | > 130 | > 20 | > 2500 | > 700 |
| 99.5% Al ₂ O ₃ | 100 | 25 | 620 | 360 |
| PSZ | 48 | 6 | 1880 | 360 |
| ZrO ₂ -Y ₃ | 1.2 | 0.8 | 68 | 30 |
| SiC | 8.9 | 1.5 | 150 | 22 |
| Si ₃ N ₄ | 0.37 | 0.17 | 7 | 1.1 |
| TiB ₂ | 15 | 2.4 | 270 | 48 |
| B ₄ C | 0.97 | 0.37 | 3.7 | 2.0 |
| SiSiC | 2.5 | 0.5 | 150 | 27 |

The Carbon steel (C-steel) as the reference material, was reported to show a ductile erosion behaviour at maximum impingement angles ranging from (15° to 30°) and of course depending on impingement velocity, while the erosion rate displays low dependency of impact angle ranges of (15 to 45°), which shows a weight loss of (50 to 60 %), maximum recorded at the (90°) with a strong dependence of velocity of which

(Tilly, 1979) and (Raask, 1969), was adopted and it takes the form as:

$$E = MpKF(\alpha)V_p^n$$

Were,

E = Weight loss of the target material

M_p = Mass of sand hitting the target material,

V_p = The particles impact velocity

α = Particle impact angle

K and n = constants, that are assumed to be depended on the physical characteristics of the materials,

F(α) = A function relationship describing the erosion wear rate dependency of the impact angle.

And the relative erosion resistance, (REF) of materials for the experiment was determined by the following expression as:

$$REF = \frac{\text{Volume loss material}}{\text{Volume loss of the reference c-steel}} \text{-----(2)}$$

The test results are presented in (Table 1) below, for weight loss per kilogram for sand impact of the tested materials.

exponent is up to (2.6) that is also reported by other researchers. The other standard materials tested as shown in the above table 1, (316- steel), duplex stainless-steel was reported to show ductile behaviour including the nickel coatings. The erosion wear rate of the standard steel materials volume loss when compared with the reference material as illustrated in (Figure 3.1) below:

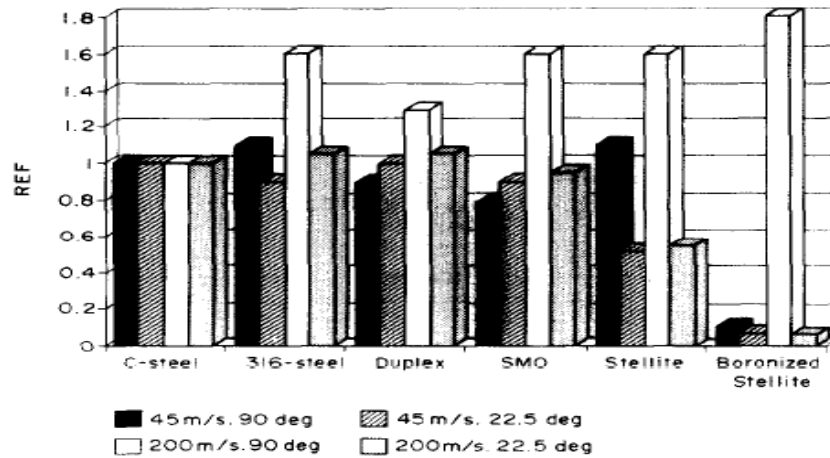


Figure 3.1: Erosion Rate of the steel qualities relative to C-Steel (Haugen et al, 1995).

The highlight inferred from the above case study is that, the stellite alloys including the boronized-stellite shows brittle behaviour as shown in the test results. However, it is noted that, impact angle variation during the testing process was not sufficient enough to extensively determine the exact ductility of these materials therefore, one might misinterpret some of the results as shown in the (figure 3.1) above as brittle materials behaviour at the higher velocity of impact. Looking at the chart, it is clear that almost all the stand steel grades materials displays similar erosion wear resistance which variation was less at angle (22.5°) for just (10%) and (60%) at the maximum angle of impingement (90°).

For all the materials, only the boronized-stellite with hardness value of (1500HV) demonstrated significant improvement in its erosion wear resistance by (10%) when compared with the standard stellite with hardness value of (400HV). The hard cover layer however, was reported to crack which fall off at higher velocity that resulted in ‘catastrophic erosion wear (Haugen et al, 1995); and the model results when compared with the experimental result shows a respectable accuracy this is restricted to the erosion attack location and magnitude of the rate of erosion wear which of course demonstrated that improvement can be achieved (Haugen et al, 1995).

Conclusively, according to the researcher, it was observed that (SEM) examination of the eroded surface, the test materials shows that erosion wear rates is significantly associated with cracking of the carbide-particles and the binder materials that resulted in the falling off of the individual carbide specks and the binding materials between the grains of the tungsten carbide and ceramic quality materials were not broken to the same range when compared with the lesser erosion wear resistant materials test (Haugen et al, 1995).

1.4 Case 2: Experimental Investigation of erosion of stainless steel by liquid-solid Flow Jet Impingement (Yao et al, 2015)

Several experimental investigations into erosive wear damage in various materials have been carried out in the oil and gas industry over the years. More recently, (Yao et al, 2015) investigated erosion wear on Austenitic stainless steel (304 and 316), 20m/s high jet velocity ejected through a 13mm nozzle with varying impingement angles of 20° – 45° respectively. The chemical composition of the two stainless steel 304 and 316 is has shown in the (Table 2) and the experimental set-up for the test apparatus is as shown in (Figure 3.2), below:

Table 2: Chemical composition of stainless steel 304 and 316 (Jun Yao et al 2015)

| type | composition (concentration) % | | | | | | | | | | |
|--------------------------------|-------------------------------|------|-------|-------|------|-------|-------|--------|--------|---------|--------------------|
| | GB1220-84 | AISI | C | Si | Mn | Ni | Cr | S | P | Mo | others |
| austenitic stainless steel No. | Ocr18Ni9 | 304 | ≤0.08 | ≤0.75 | ≤2.0 | 10-12 | 17-19 | ≤0.020 | ≤0.035 | – | B≤0.0015 N≤0.05 |
| | Ocr18Ni12Mo2 | 316 | ≤0.08 | ≤0.75 | ≤2.0 | 10-14 | 16-18 | ≤0.030 | ≤0.040 | 2.0-3.0 | – |

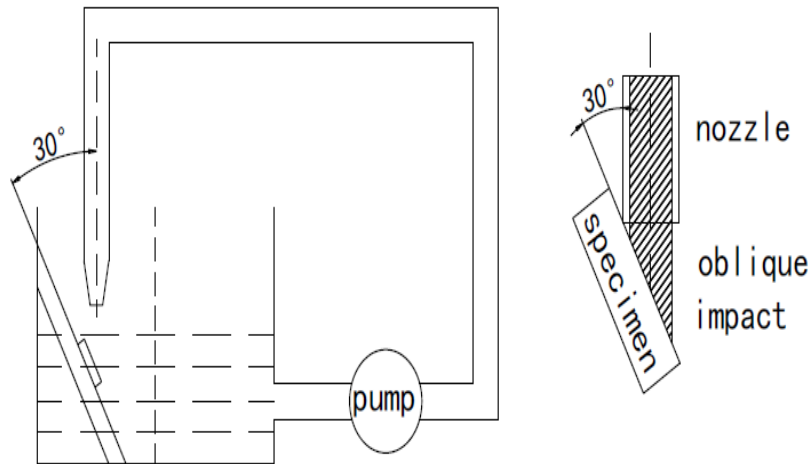


Figure 3.2: Schematic of the Jet Impingement erosion experimental set-up (Jun Yao et al, 2015)

The experiment shows that stainless steel (306 and 316) mass loss per unit area at 30° impingement angle and tap water with (0.2 wt. %) quartz sand (0.18mm) has a functionality of the test time. The test was also conducted with sea sand (0.18mm), (0.07wt. %) tap water and 30° impingement angle. It is observed that both of the two steels used for the test follows a linear relationship with regard to the mass loss per unit area independent of the varying effect of the sand and indicated steady erosive wear for the jet impingement erosion test. However, stainless steel 304 erosion rate was observed slightly higher than 316. This may be an indication for the presence of the molybdenum (Mo) element in the stainless steel 316, which is observed as the main dissimilarity between the two steels.

The presence of molybdenum in materials increases hardness against indentation which has also been seen by other researchers as a decisive effect on erosive wear resistance in the industrial equipment. Figure 3.3 (a) represents mass loss per unit area of (stainless steel 304) in (0.15wt. % tap water), (0.25mm quartz sand and sea sand) and 30° impingement angle respectively as a function of test time.

There still appears a linear relationship of mass loss rate per area with time in the experiment irrespective of the varying sand effect under the same jet impingement conditions. However, the quartz sand eroded more material than the sea sand because of the fact that quartz sand is harder and more angular shaped than the sea sand as shown in the graph and microscopic (SEM) images as illustrated in (Figure 3.3) below:

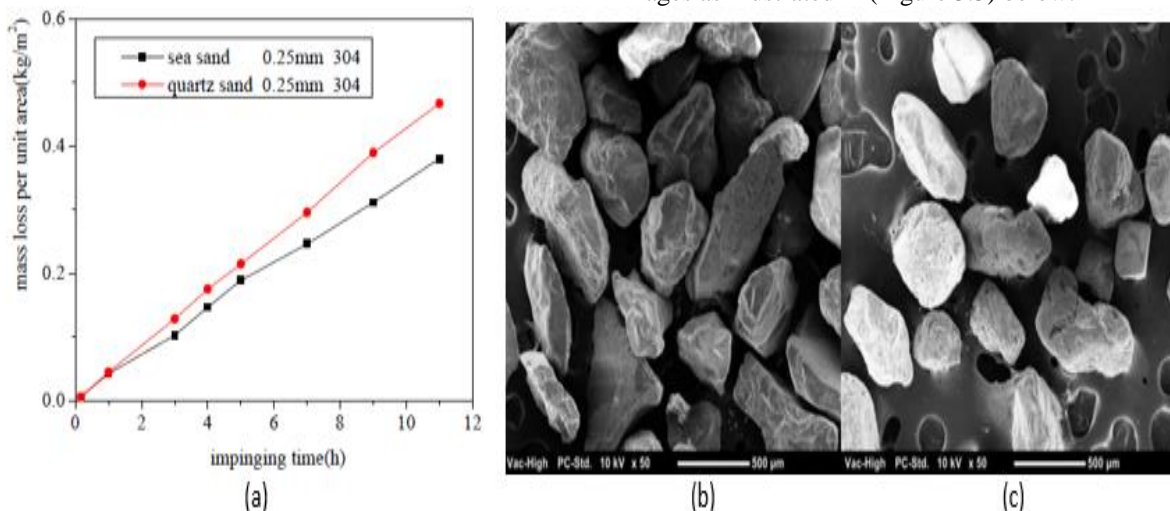


Figure 3.3: (a) Shows the graph of mass loss per unit area versus impingement time and SEM photos of (b) quartz sand and (c) Sea sand respectively (Jun Yao et al 2015)

A graph of mass loss (per unit area) of the stainless steel-316 with respect to the impact angle of (60°) in the tap water containing the erodent sea sand with

particles size of (0.1wt% and 0.07wt%) correspondingly as a function, versus test time was plotted as illustrated in (Figure 3.4) below: Equally, as

can be seen in the graph, (mass loss rate per unit area) steadily increased with the impingement time before (15hs) in the stainless steel-316 which indicated that

the erosion wear rate of stainless steel-316 increases with respect to test time in this alloy.

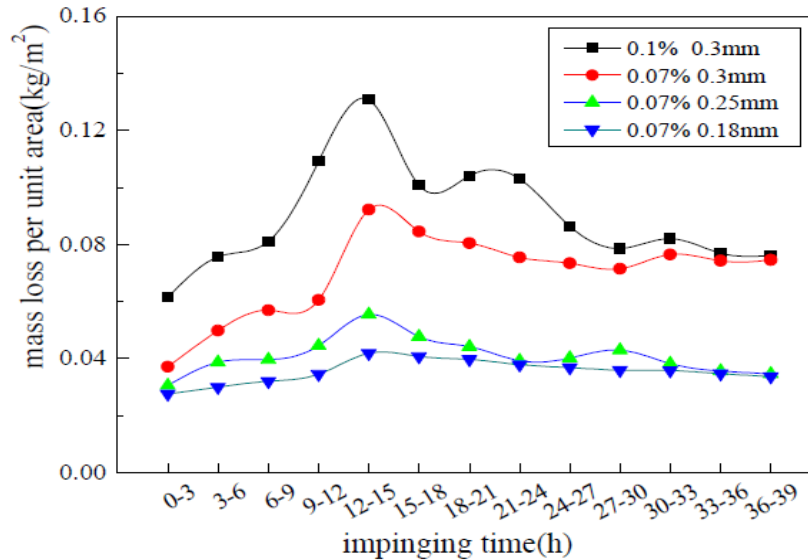


Figure 3.4: Shows the mass loss per unit area versus impingement time (Yao et al, 2015).

The erosion rate as can be seen in the above graph is observed to be at its maximum with the (12 – 15hrs) with maximum mass loss per unit area roughly about (0.14kg/m²) then erratically reduced to a certain constant value which is seen from the graph has been common in all the sand size and concentration also reported by (Yao et al, 2015). However, they reported that larger particles size and concentration were observed to cause more erosion effect on the test target materials and were unable to identify the mechanism behind this effect. One could suggest at this point that, this could be due of the oxidation process or due the low carbon composition (0.08wt %) of the stainless steel-316 and the impingement angle of (60°) used for the test. On the other hand, they also, did not ascertain the level of conformity of their test with numerical model and compare their result with similar experimental research done in the past to ascertain points of correlation.

1.4.1 SEM Analysis of the Target Material- (Stainless Steel 304, and 316) Surface Morphology

They also, conducted a Scanning Electron Microscope (SEM) analysis of the two austenitic (stainless steels-304 and 316) surface morphologies, and observed their behaviour under the test conditions and reported that, after (10minutes) of the test for (stainless steel-304) for example, the target surface of the material seriously damaged and identified that the grain boundaries became illegible, and an increment of the exposure time from (10minutes) to just (2hours) shows that, the target material surface does not only completely damaged, but also, there is a significant development of the additional fluctuation and severe plastic distortion and fractures of the target material surface, (Yao et al, 2015).

This degradation phenomenon was also observed in the previous works of (Lee and Kim, 2002). Also, as can be seen illustrated from (Figure 3.5) (b), increase in the impingement energy of the tangential component produce micro cutting and ploughing with accompanied chips-lips that will eventually detached through further successive particle indentation, which will cause more material removal that was also observed in the works of (Bitter, 1963).

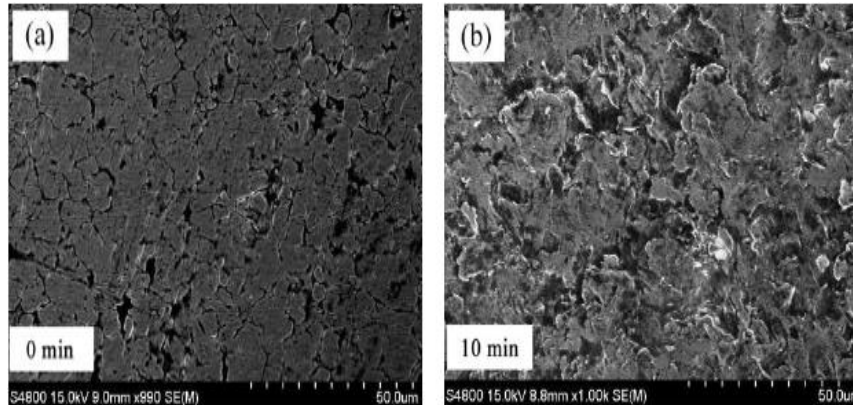


Figure 3.5: (The surface morphology of stainless steel-304 :(a) before test, (b) test after (10minutes) of particles impingement time (Yao et al, 2015).

The SEM surface morphology result displays similar damage mechanisms in their study and the stainless-steel grade-316 tested, which contains up to (2.0 – 3.0wt %) of the erosion wear resistance element (molybdenum).

Mostly apparent are flow shape indentation generated by the severe plastic-distortion at oblique impingement and the damaged target material surface consist of thin dishes of fractures, and the material cutting mode of deformation is observed predominant at minor impaction angles. An extruding cutting gesture is seen in the direction of the impinging particles when the indentation particles scratched on the material surface as scar chip-lips that will be fatigued by subsequent particles impingement actions and in such cases, the transverse cutting stress is observed rather than normal pressure-stresses according to (Hu, Zhen, and Qin, 2010).

From (Figure (3.6) below, it is apparently clear that crater-grooves are formed on the target material surface. This mechanism was corroborated by the works of (Neilson and Gilchrist, 1968), that solid erodent particle indentation on target material surface with higher velocity could lead to pressure on the impacted spot, and extrusion of the material around the resultant-craters could be randomly positioned, and this action was caused by subsequent particles impingement that will eventually fracture, as also cited in the works of (Ninham, 1988).

According to (Misra and Finnie, 1981), the erosion wear mechanism of erodent-sand particles of these (stainless steels-316) in a carrier-fluid causes deformation on the surface exposed to the slip-band creation due to the mechanical actions of kinetic-energy transferred to the surface of the material, as can be seen in figure 3.6 below:

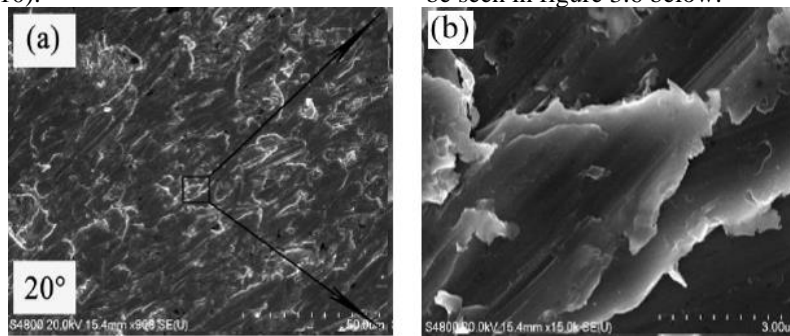


Figure 3.6: SEM surface analyses on stainless steel-316 after 2hours exposure: (a) before and (b) after the test (Yao et al 2015)

1.4.2 Model for Wear Prediction/Coriolis Wear Test

Tian *et al* (2005), presented a model for predicting the sliding wear rate to be computed as a ratio of friction power of the particle to the specific energy of wear for somewhat specified slurry wear material combination. The sliding wear equation is presented as:

$$\dot{W}_S = \frac{P}{Esp}, \text{ and the friction power (P) is given as:}$$

$$P = \tau V_t \text{-----(3)}$$

Were,

$$\dot{W}_S = \text{sliding wear rate}$$

P = friction power

Esp = specific energy of wear slurry/material

τ = shear stress between the particulate

phase and the wear surface

$V_t =$ tangential velocity of the particles

Once the friction power exceeds certain critical values, particle erosion will take place.

Based on simplified assumptions, the Coriolis wear test average values for the specific energy are calculated by the following equation:

$$Esp = (\rho_S - \rho_L)\Omega^2 R_m C_0 \left(\frac{Q}{b}\right) \left(\frac{1}{W_S}\right) \text{-----(4)}$$

Were,

ρ_S and ρ_L

= densities of the solid particles and the carrier liquid respectively

$\Omega =$ angular velocity of the Coriolis channel

$R_m =$ mean radius (from the axis of rotation of the channel)

$C_0 =$ delivered slurry concentration by volume

$Q =$ Volumetric flow rate

$b =$ width of the channel

It is worthy to note that, the wear rate can be estimated from mass loss measurement or otherwise, from computation fluid dynamics (CFD) computation of the local shear and velocity and thereafter, use the actual local wear depth from experiment to estimate the specific energy locally, (Tian *et al*, 2005).

However, in practice, it is observed that the specific energy considerably depends on the particle sizes (Oka, 2009). To avoid this, using relatively narrow banded sand particles for the test is recommended (Tian *et al*, 2005). The objective will be to examine the effects of particle size regarding wear by choosing the sim-narrow grade sand/copper slurry particle sizes ranging

from 15 - 2040 μ m as the (D50) sand grade. The highlight of the test shows that, the Cr – Mo material demonstrated the greatest wear resistance and specific energy in all the four particles size used for the Coriolis wear test.

1.4.3 The Influence of Temperature on Erosion Wear

Suur, (1962), cited in the works of (Kleis, 2008: p36-43), conducted comprehensive research into the temperature influences on the erosion wear rate using a distinctive pneumatic test rig and reported a detailed explanation on the test proceeding in his work. The test rig tolerates the pre-heating of both the erodent abrasive particles-quartz sand, and the acceleration gas (argon), and the test target material-test piece at the same time.

The plate shaped test piece (4mm) that contains a (20 \times 20mm) wearable-surface, was passed through with a current of (1200A) supplied by a low voltage transformer. In other to completely avoid oxidation action in the test piece during the experiment, an aperture was created in the test piece, and a thermos-junction was attached to the test piece surface except the wearable-surface which was chromium- plated. In other for maintenance of stability of the temperature, the test piece was supplied electricity with a special device automatically as the test proceeds.

The main focus of the test was to determine the ‘change in erosion wear rate with respect to temperature typically experienced in chemical plants and power, and simultaneously, modifying other erosion wear parameters engineering’ (Kleis, 2008).

It is illustrated in (Figure 3.7) below, that the rate of wear at the preliminary phase as observed are seen not to be continuous, and can be said not being eroded (wearing).

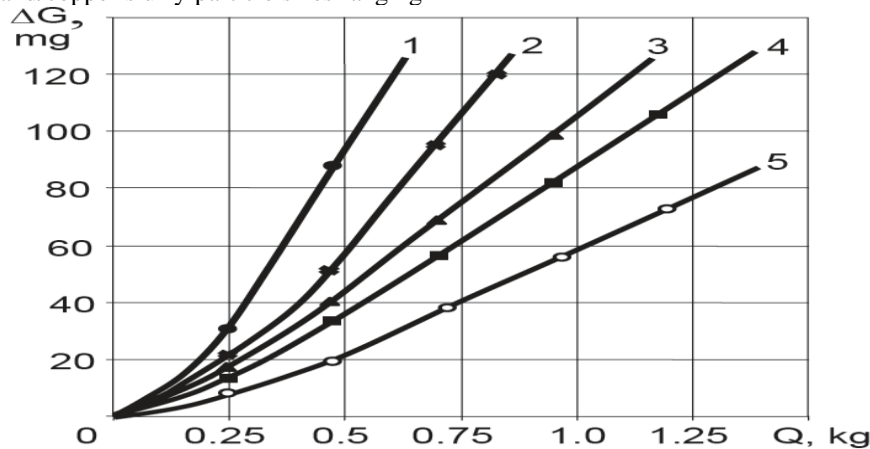


Figure 3.7: Weight loss dependence ΔG on the amount of quartz sand attacking the target piece, $v_o = 48\text{m/s}$, $\alpha = 90^\circ$, erodent sand size 0.4 - 0.6mm: 1 – steel St3, 2 – steel 45, 3 – U10A, 4 – R9, 5 – cast iron Ch34L (Kleis and Kulu, 2008).

Suur used five different materials for the test to determine the dependence amid the temperature effects on the materials erosion wear rate. The chemical

composition of the five material is as shown in (Table 3) below:

Table 3: Shows the chemical composition of the material tested by Suur, cited in the works of (Kleis and Kulu, 2008).

| Material symbols (Russian standard) | Mean of constituent elements, wt% | | | | | | | | |
|--|-----------------------------------|-------|-------|-------|-------|-----|-----|-----|------|
| | C | Si | Mn | Cr | Ni | Ti | V | W | Mo |
| Steel St3 | 0.2 | ~0.2 | ~0.5 | | | | | | |
| Steel 45 | 0.45 | 0.25 | 0.6 | <0.25 | <0.25 | | | | |
| Steel U8A | 0.8 | 0.2 | 0.2 | <0.15 | | | | | |
| Steel U10A | 1.0 | 0.2 | 0.2 | <0.15 | | | | | |
| Steel 9Ch | 0.9 | 1.4 | 0.5 | 1.0 | | | | | |
| Steel 1Ch13 | <0.15 | <0.6 | <0.6 | 13 | <0.6 | | | | |
| Steel Ch17 | <0.12 | <0.18 | <0.7 | 17 | <0.6 | | | | |
| Steel R9 | 0.9 | | | 4 | | | 2.3 | 9 | <0.3 |
| Steel R18 | 0.75 | | | 4 | | | 1.2 | 18 | <0.3 |
| Steel 1Ch18N9T | <0.12 | <0.3 | <2.0 | 18 | 9 | 0.8 | | | |
| Steel 5ChV2S | 0.5 | 0.6 | 0.3 | 1.2 | | | | 2.2 | |
| Steel Ch12F1 | 1.3 | <0.4 | <0.25 | 12 | | | 0.8 | | |
| Cast iron Ch34L | 2.0 | 1.5 | 0.7 | 34 | | | | | |

Form the graphs as illustrate in (Figure 3.8) below, at temperature range of (400 – 450°C), erosion wear rate of the materials hardly shows any change, and rather even observed to be decreasing in some of the materials (e.g., carbon steel specifically at the (90°) impingement angle).

However, it is observed that the CH34L alloy maintains strength of stability at about (500°C), and all the other material are observed to show sharp-increase in their rate of erosion wear at the temperature of (450°C), except the Ch34L which demonstrated a ductile behaviour.

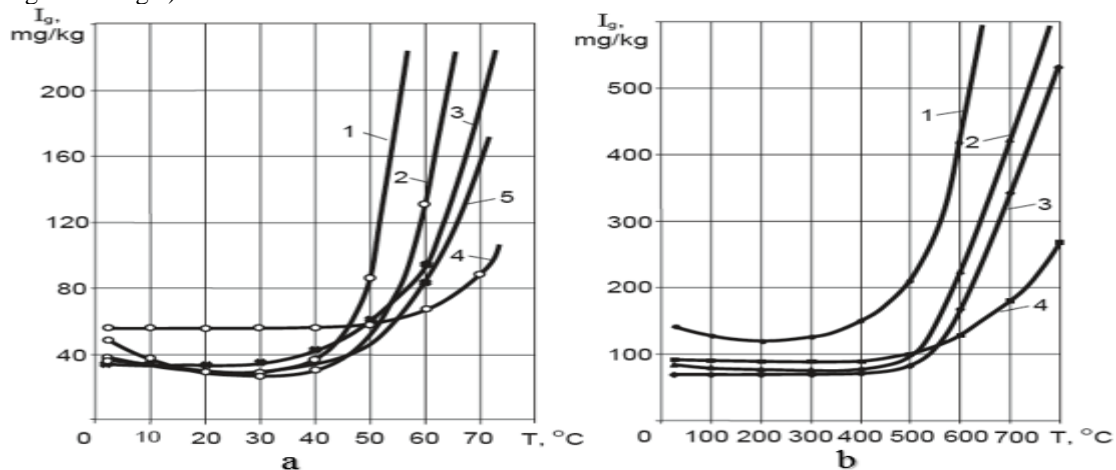


Figure 3.8: Shows the Dependence of erosion wear rate I_g on temperature T at (a): impingement angle of 45° , and (b): impingement angle of 90° with velocity of 48m/s, quartz-sand 0.4 – 0.6mm: 1 – steel St3, 2 – steel U8A, 3 – steel R9, 4 – cast iron Ch34L, 5 – steel 9ChS ((Kleis and Kulu, 2008).

This ductile behaviour of the Ch34L alloy, is not unconnected to the influence of the ‘oxide films that are emerging on the surface of the target material during the process of erosion wear’ (Suur, 1962). It was also observed that the temperature increases also, go together with rapid growth of the film, and due to the exterior layer (Fe_2O_3) Vickers hardness of (Ca 1140HV), which act as a protective coating at the

temperature of around (450°C). Further increase in temperature around (570°C), the film consisting three layers, of which the weakest (FeO) combined with the bulk material instantaneously, which is the reasons for the steep rise in the rate of the erosion wear in the materials.

Another fundamental parameter examined by (Suur, 1962), was the influence of **the particle’s**

impingement angle. This was tested on four target materials and it was observed that the ‘critical angle’ which is at (30°) for steels at lower-temperature (room), which is observed shifting to around (45°) at higher temperatures but cast-irons maintains the same angle (45°) even at higher temperatures.

The results of the **relative volume erosion wear resistance (ε)** of the test are presented in four different stages and the influence of the particles erodent velocity for three other materials are of a velocity range of (48 – 70m/s), as illustrated in (Table 4) below:

Table 4: Relative volume erosion wear resistance of materials in a stream of 0.4 - 0.6mm quartz sand in relation to reference material - steel St3 at the mean velocity of particles 56m/s and velocity exponent m at 5000C, fraction of sand 0.4 - 0.6 (Suur, 1962)

| Material | Hardness ^a HV | Relative erosion resistance ε at | | | |
|----------|-----------------------------|----------------------------------|----------------|----------------|----------------|
| | | 20°C, α = 90° | 600°C, α = 90° | 600°C, α = 45° | 700°C, α = 90° |
| 45 | 185 | 1.1 | 1.2 | 1.3 | 1.4 |
| USA | 190 | 1.2 | 2.1 | 1.6 | 2.0 |
| U10A | 197 | 1.2 | 2.5 | 1.8 | 2.4 |
| 9ChS | 210 | 1.2 | 3.4 | 2.3 | 3.4 |
| 5ChV2S | 230 | 1.3 | 3.6 | 2.1 | 3.1 |
| 1Ch13 | 160 | 1.1 | 3.6 | 2.1 | 3.1 |
| Ch12F1 | 240 | 1.2 | 3.9 | 2.5 | 4.1 |
| Ch17 | 160 | 1.1 | 4.2 | 2.4 | 4.6 |
| R9 | 240 | 1.3 | 3.5 | 2.5 | 3.7 |
| R18 | 230 | 1.4 | 3.9 | 2.6 | 4.9 |
| 1Ch18N9T | 160 | 0.9 | 4.5 | 2.5 | 5.3 |
| Ch34L | 290 | 0.9 | 4.1 | 2.5 | 5.5 |

| Material | Impact angle | |
|----------|--------------|---------|
| | α = 30° | α = 90° |
| R9 | 2.6 | 2.6 |
| 5ChF2S | 3.0 | 3.5 |
| Ch34L | 2.5 | 3.2 |

Remarkably, amongst other conclusion deduced from this case studied is that: In studying the mechanism of ripples emergence and requisites for its development processes, one could suggest that it is due to the straight malleable distortion instigated by the particle’s impingement. There is a need for exhaustive erosion wear elevated wide range of temperature testing to identify the rate of particles impact velocity and particles impingement fluctuation to validating the erosion wear oxidation and reveal any inadequacy. This is to improving our knowledge of the erosion wear oxidation interactions of materials. Also, observed from the present case studied, the formation of the ripples actually initiated the early plasticity behaviour of the target material which was before the increase in the velocity of impingement. However, the reason for this behaviour of the target material is not clear.

Lately, introduction of computer simulation in investigating erosion wear has advanced the frontiers of erosion wear research studies and given an innovative outlook to the erosion problem. Application of computer simulation coupled with numerical analysis has steered ‘deep and comprehensive investigations’ into the erosive wear mechanism and results obtained through this approach are very promising (Kamran, 2010).

Researchers, such as (Arabnejad *et al*, 2015), have developed quasi-mechanistic erosive wear equation which combine methods of empirical models that captures erosive mechanism which provides substantial agreement when compared with data obtained experimentally and computer CFD simulation data. The model equation final formula is as shown below:

1.4.4 Computer Simulation and Analytical Model of Erosive Wear

$$ER_C = \begin{cases} C_1 F_s \frac{U^{2.41} \sin(\theta) [2K \cos(\theta) - \sin(\theta)]}{2K^2} & \theta < \tan^{-1}(K) \\ C_1 F_s \frac{U^{2.41} \cos^2(\theta)}{2} & \theta > \tan^{-1}(K) \end{cases}$$

$$ER_D = C_2 F_s (U \sin \theta - U_{tsh})^2 \quad \text{-----(5)}$$

Were,

$C_1, C_2, K,$ and U_{tsh} = Empirical constants

F_s = particle sharpness i.e., for (sharp particles is, 1), (semi-rounded particles is, 0.5) and (fully rounded particles is, 0.25), (Arabnejad *et al*, 2015).

$ER_C + ER_D$ = Total erosion

(Table 5) below, shows the empirical constant for seven materials tested with the model equation.

Table 5: Empirical constants for the erosive wear model equation (Arabnejad *et al*, 2015)

| <i>Material</i> | C_1 | C_2 | K | U_{tsh} (m/s) |
|----------------------|----------|----------|-----|-----------------|
| Carbon steel 1018 | 5.90E-08 | 4.25E-08 | 0.5 | 5.5 |
| Carbon steel 4130 | 4.94E-08 | 3.02E-08 | 0.4 | 3.0 |
| Stainless steel 316 | 4.58E-08 | 5.56E-08 | 0.4 | 5.8 |
| Stainless steel 2205 | 3.92E-08 | 2.30E-08 | 0.4 | 2.3 |
| 13 chrome steel | 4.11E-08 | 3.09E-08 | 0.5 | 5.1 |
| Inconel 625 | 4.58E-08 | 4.22E-08 | 0.4 | 5.5 |
| Aluminum alloy 6061 | 3.96E-08 | 3.38E-08 | 0.4 | 7.3 |

However, there are some levels of uncertainties in the experimental data (weight loss and velocity measurement) for the impingement test as shown in (table 5) above. These errors are due to the particles being accelerated by gas and measurement errors of the particles image velocimetry (PIV) and the gas velocity measurement by Pitot tube, (Arabnejad *et al*, 2015).

1.4.5 Erosion wear in Choke valves and Separators

Choke valves and separators are critical equipment's in the oil and gas industry, that is complex, and unique with highly sophisticated operations that needs materials of higher qualities, which can withstand the rigors of extreme engineering application, and enduring environmental conditions (Nokleberg and sontvodt, 1995).

The complexity of the operating conditions, and parameters that contributes to erosion wear discussed earlier needs to be considered when making decision for selecting suitable materials for any given engineering application.

1.4.6 Erosion Wear in Choke Valves

Production of solid particles with hydrocarbon in oil fields usually causes severe erosion wear in surface equipment such as choke valves which mostly operate at sonic velocity (Haugen *et al* 1995). Choke

valves are typically situated on well heads specifically to balance/control pressure of the hydrocarbon flowing into a manifold so as to protect the equipment from experiencing unusual fluctuation of pressure drop.

Huge pressure drops in the well stream that contains multiphase fluid flow with accompanying solid particles can reach up to (450 and 520 m/s) (Neilson and Gilchrist, 1968); which could produce heavy metal erosion wear rate due to the solid particles impingement, cavitation, liquid-droplet and the combined phenomenon of erosion and corrosion that can lead to the reduction of the choke valves operating lifetime (Ninham, 1988). Erosion wear can cause severe damage to valve seating-surface which can invariably compromise the choke valve shut-off and obstruct the valve control performances in operation.

Severer erosion wear cases can result to the valve failure and even breach off the valve 'pipe pressure boundary' (Roth, 2001). Generally, in typical hydrocarbon production condition in unconsolidated sand producing reservoirs, frequent choke valves replacement in the ranges of four to eighteen months may occur (Akbarzadeh *et al*, 20120). In the North Sea for example, there are reported cases of choke valve critical parts been completely damaged by erosion wear in a matter of hours in operation (Haugen, 1995), as shown in (Figure 3.9).

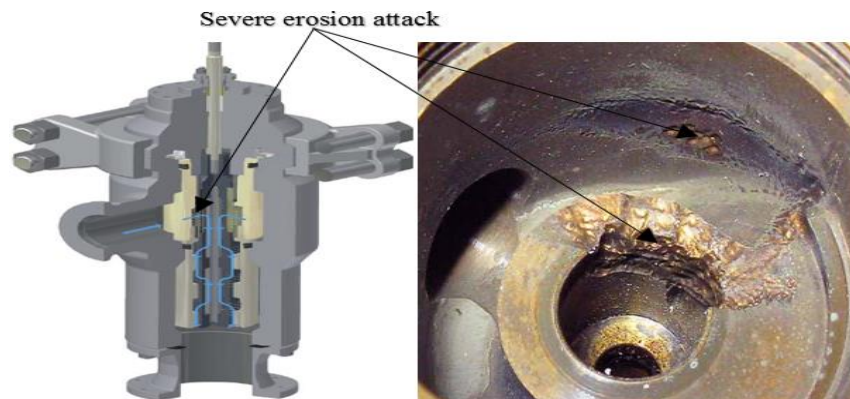


Figure 3.9: Severe erosion wear attack on choke valve observed in the North Sea (Courtesy: Kent Introl Ltd., 2009)

Eroded choke valve replacement is accompanied with greater costs and adverse safety implications. With hydrocarbon (oil and gas) production moving into deep and extreme subsea environment, with higher consequential cost effects, increasing the service life of the choke valve could significantly lead to reduce cost and reduce safety concerns. Though erosion damages in surface production equipment in some cases are considered inevitable situations (Arabnejad *et al*, 2015). Choke valve design optimisation, and proper erosive wear resistance material solutions would significantly reduce the erosion of such equipment due to flashing and cavitation erosion.

1.4.7 Flashing Erosion

Figure (3.10) illustrates, a typical damaged choke valves plug due to flashing erosion wear in the

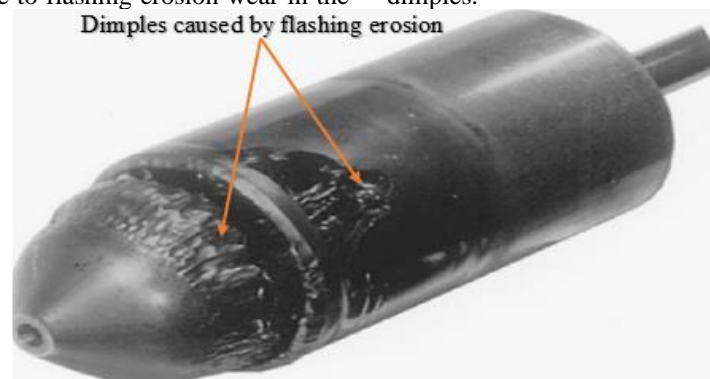


Figure 3.10: Valve plug damaged by flashing erosion wear (courtesy: Fisher Controls International, Inc., 2004).

However, to reduce or completely eliminate flashing erosion requires the modification of the valve design or the operating system particularly, either the vapour pressure of the system or the downstream pressure. Some systems cannot be easily altered; therefore, modification might not be an option for such systems. Other consideration could be the relocation of the valve position and the hardening of the valve trim with advanced materials which is a more reliable solution.

North Sea. Flashing erosion of choke valves is prevalent in liquid application due to the downstream pressure lower or equal to the vapour pressures of the liquid. Whenever there is restriction in flow, the decrease in pressure can cause the fluid to reach the fluid vapour point. Flashing occurs when the fluid vaporises and remain a vapour as it flows downstream. The generated vapour bubbles at the vena contracta remains unbroken and un-collapsed because the pressure recovery is highly sufficient. As soon as flashing occurs, the downstream fluid been a mixture of (vapour and liquid) that is moving with relatively high velocities, subsequently causing erosion in the valve material and the immediate walls of the pipe downstream (skousen, 2004). Metal erosion caused by flashing appears smooth and shining and some form of dimples.

1.4.8 Cavitation

Cavitation as defined in the ASTM G32-03 standard, as the formation and subsequent collapse, within a liquid, of bubbles or cavities that contains either vapour, gas or both at the same time (ASTM, 2005), and (Hattori and Mikami, 2009).

Cavitation damage in choke valves occurs when the fluid vaporises then returns to a liquid state at the

processing conditions as pressure increases downline. The metal damage caused by cavitation appears to be

rough and irregular due to pitting of the surface as shown in (Figure 3.13).



Figure 3.11: Cavitation erosion wear damage of a globe valve trim (Sotoodeh, 2015).

Cavitation is a major source of damage in control valves and other components (Al-Bukhaiti et al 2016). It occurs as the liquid passes through a restriction such as a valve. The restriction causes the liquid velocity to increase and its pressure to decrease. The point of maximum velocity and minimum pressure is called the (vena contracta).

Liquid micro jets form when the recovering pressure makes indentation in the bubble then the micro jet burst through the bubble. These implosions

can also cause pressure waves up to 100, 00 lbs/in². The combination of pressure wave and micro jet can cause severe damage to the valve plug, seat and body when they are located near the material surface.

Cavitation can also cause unacceptable noise and vibration that reduce efficiency or leads to loss of process control. Even though cavitation occurs, it does not always cause damage (Fisher services, 2010).

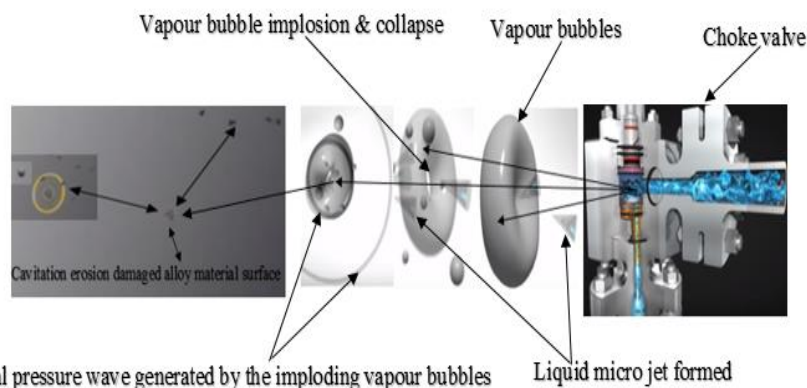


Figure 3.12: Hydrocarbon fluids cavitation erosion wear damage process in choke valves (Courtesy: Fisher services, 2010).

Though, equally liquid droplets and particle impingement and cavitation damage material surfaces through over-pressure, the mechanisms of cavitation erosion wear basically varies from the impaction mechanisms. In cavitation fluid flows, shockwave or entrant liquid micro-jet formed through rapid vapour-bubbles collapse produce very elevation localised-pressure (Arefi and Angman, 2006).

If the bubbles collapse occurs exactly or near the material surface, the generated high-pressure stresses

will plastically deform the valve material walls. In due course, sufficient cavitation actions will result to the surface failure that leads to surface-pitting shape which is symbolic to cavitation erosion wear. The further frequently the cavitation occurrence, the more rapidly the erosional damage grows (Roth, 2014).

Factors affects the rate of cavitation erosion in choke valves are: The intensity of the cavitation, the materials used in the construction of the area where the cavitation occurs – Hardened materials reduces erosion

cavitation damage. The length of exposure of the material surface to cavitation erosion – The more frequently that cavitation erosion wear occurs in an area, the more likely it is to sustain damage (Ashby and Cebon, 1993).

Generally, when cavitation begins near a surface, it will certainly cause damage to the surface. Materials with high toughness can intensely slow the damage rate due to cavitation erosion. But such materials too will in due course yield to cavitation erosion damages (Roth et al, 2001).

Hydrocarbon fluid temperature will also, affects cavitation damage prospective, mainly because engineering materials properties tends to vary as a function of high temperature (Bellman and levy, 1981). Cavitation also, tends to accelerates prevailing corrosive mechanisms, underpinning the need for advanced material solutions for corrosion resistance in

potentially cavitation prone oil and gas applications. (Atapek and Fidan, 2015).

1.4.9 Erosion wear in separator

In all oil and gas processing facilities, contamination of internal walls and component is a realism that is linked with numerous complications, and if not properly handled, could degenerate to other environment issues. Erosion mechanism in separators internal walls and component is not clear rather than the effect of sand and other solid particles deposition (Henni, 2013). However, it is reasonable to think that solid particles impingement can, and does occur in the inner component of the separators such as inlet deflectors and other critical components of the separator as shown in the (Figure 3.16) below.

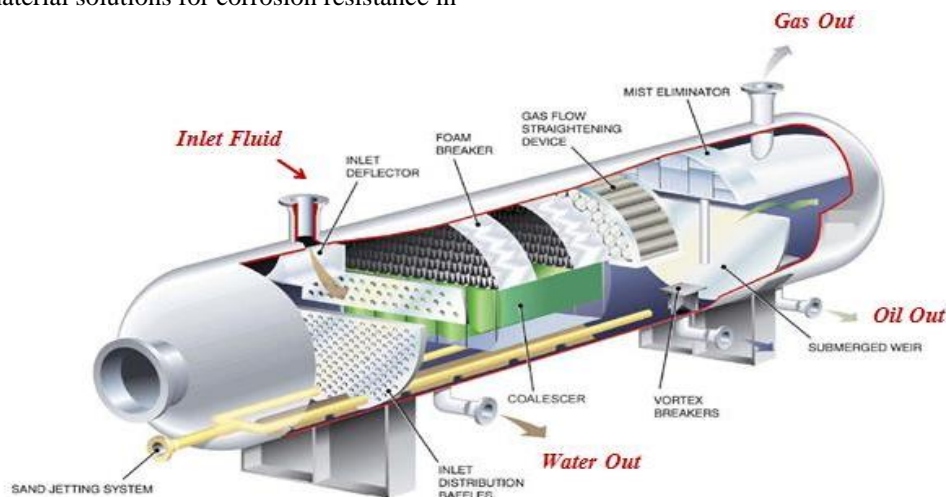


Figure 3.13: A typical oil and gas three phase horizontal separator with complete internals (Engineering, 2014).

Predominantly, erosion-corrosion effect is more associated with hydrocarbon separators due to the corrosive fluid such as (CO₂ and (H₂O) presences in the fluid (Kleis, 2008). This corrosive fluid causes the surface material degradation of the internal components. Some of the failure mechanism/effects attributed to contamination in separators are: Solvent degradation, solid particles deposition, fouling and foaming, downstream impacts such as sulphur recovery units, and treated product storage units (Kraus, 2011).

These aforementioned problems if not carefully handled could lead to reduction of production capacity, decay in efficiency, failure of critical equipment, high operational and maintenance cost and ultimately, leads

to undesirous environmental degradation (Levy, 1995). However, most of these disadvantageous effects could be reduced by means of proper control mechanism and ultimately proper material solutions (Facilities, 2014). Furthermore, separator vessels can be classified based on functionality and requirement in the oil and gas industry as two-phase separators (vapour-solid separator, liquid- liquid separator, liquid-solid separator, and vapour-liquid separator), as illustrated in (Figure 3.20) below, and three phase separators (Levy, 1995). Separators are geometrically, designed mostly as horizontal, spherical and vertical, of which the vertical and horizontal configurations are commonly used in the oil and gas industry.

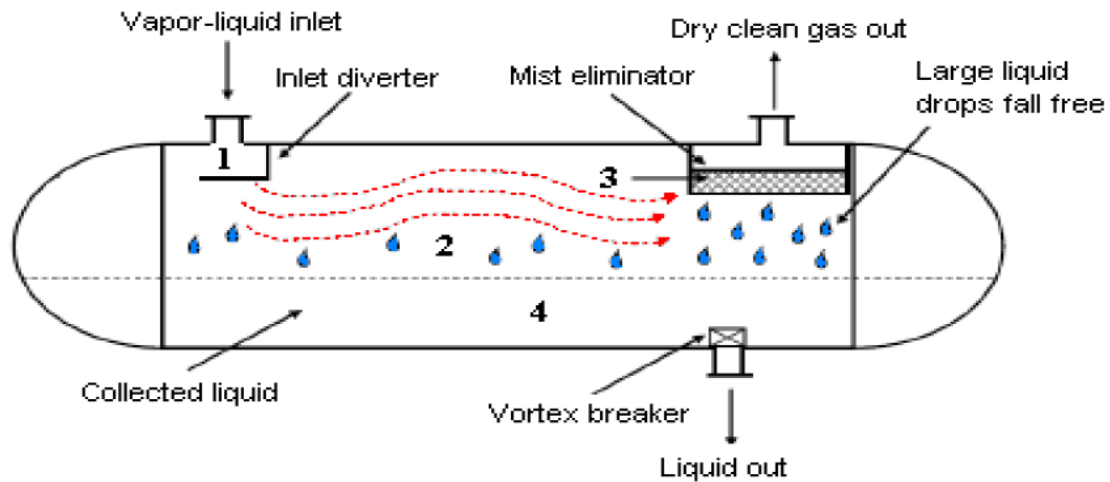


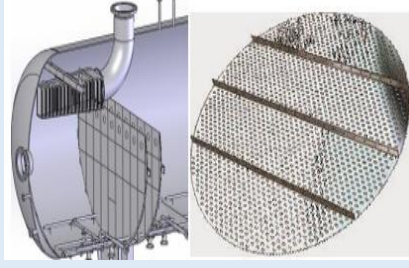
Figure 1.24: Major components of the horizontal separator and separation processes (courtesy: KLM Technology, 2011).

The main separator internal component of interest in this study is the (**inlet diverter**), which is observed to be the first contact target materials with the produced hydrocarbon fluid mixture- (oil, gas, water and solid particles), as it enters into the separator.

The inlet diverter causes the gross separation of vapour-liquid as the multiphase fluid flows into the separator and hits the inlet diverter surface, which causes sudden change in momentum when the fluid

moves into the separator. The main function of the inlet diverter and other internals, among other things, is for reduction of inlet stream momentum, enhancement of liquid-gas flow distribution, and prevention of droplet shattering that can cause cavitation erosion wear (Cousens (1984), and (Kirkprocess.com, 2016). (Table 6), shows some of the geometry of inlet diverters and their functions, failure modes/damage mechanisms.

Table 6: Shows Separators internal components and their functions/failure modes/damage mechanism (Kirkprocess.com, 2016)

| Separator Internal components | Functions/Failure modes/Damage mechanisms | Component depiction |
|----------------------------------|--|--|
| Diverter/Perforated Baffle Plate | <ul style="list-style-type: none"> ✓ Induce rapid change in flow velocity and direction ✓ Particles/liquid impingent Erosion wear ✓ Erosion-corrosion ✓ Damage due to inlet fluid over pressure ✓ Stress corrosion cracking |  |

The damage/degradation mechanism of the internal component of interest as illustrated in the above (Table 6), are used in defining the main failure issues associated to the discussed internal components within the separator. Failure of the materials used in manufacturing this component will have a detrimental economic and environmental effects.

The major protective measures for these components possibly will include: Detail improvement during fabrication and fastening processes (Maleque and Salit, 2013), and Selection of design material for this component should take into consideration the temperature and size, both maximum and minimum

pressure rate, and corrosive gas such as carbon dioxide (CO₂ and H₂S) (Ashby, 2011).

IV. REVIEW OF THE STELLITE ALLOYS MATERIAL REQUIRED FOR THE DESIGN OF THE CHOKE VALVE/SEPARATOR INTERNALS

Fundamentally, Stellite alloys are special kind of cobalt based super-alloys that have an extensive use in the oil and gas industry, primarily for erosive-wear resistance applications in harsh environment, (Engineering P. 2014). These alloys have excellent

solid-particles erosion, cavitation resistances, abrasive and adhesive wear resistance, and erosion-corrosion resistance in harsh subsea environments at higher temperature with an exceptional combination of tribology, mechanical, chemical and high temperature (Above 500°C) and other unique properties.

Stellite alloys consist of tungsten or molybdenum, enormous amount of chromium (27 – 32%) and small amount of carbon (less than 3wt %) as its common fundamentals which leads to carbide precipitation in a complex cobalt solid-solution in an alloy matrix as its main strengthening mechanism (Davis, 2000).

1.5 Chemical Composition of the Stellite Alloy Test Specimens

Alloy specimens A and B are fabricated by forging process which have a carbon content ranging from between 0.25 – 1.6wt.%, tungsten content of 4 – 32wt.% and chromium content of 22 – 30wt% respectively. Alloy C, D and E are centrifugal casting processed with similar quantities of carbon, chromium and tungsten contents except alloy D and E which does not contain tungsten and also contains less carbon contents of 0.35 wt. % and 0.25wt.% with molybdenum contents (11.8% and 11%) respectively. Alloy A, B and C are medium carbon stellite alloys and the others are low carbon stellite alloys. Furthermore, alloy D contains also, (2.07wt% niobium, (Nb)) which enhances the alloys performance in high temperature environments (Stephen 1990).

1.6 Methodology

The methodology that is used are within the research objectives which is the ‘mixed method’ of ‘qualitative and quantitative,’ analytical research, using both empirical data (evidence) and models obtained in the literature review to predicting the erosive wear rate, and the selected material serving as a solution in reducing/mitigating erosion wear rate.

The approach used in arriving at the results of this research is the deductive approach. This help in critically evaluating the general knowledge that exist on the subject matter (material solutions to reducing wear and erosion in oil and gas industry), and progressively narrowing down to the specific outcomes. Existing erosive wear experimental data/evidence and the analytical modelling has been critically evaluated, and the model published by Nsoesie (2013), were used to predict the erosion wear rate of the selected materials, and the results were extensively discussed.

1.7 The Adopted Experimental/Analytical Model

Based on the multiplicity of the erosion wear mechanism and parameters, a single mathematical

equation could not be able to accommodate all the parameters as observed in most of the literature reviewed. Presently, there is no ‘one model fits it all’ solution in the industry as observed from the literature reviewed.

The only visible solution always depends on the prevailing situation and the required methodology that will be best applicable to the scenario being handled at the time which will yield the desired result, is always applied for the erosion wear prediction.

However, the adopted empirical/analytical model (Nsoesie, 2013), for erosion wear prediction in this present research consists of five variables, which includes: erosion wear rate (w_1), as a function of the particles diameter (D), velocity of impact (V), density of the particle (ρ_p), target material hardness (H_v), and particles impact angle (α). Thus, the final form of the adopted model equation given by (Nsoesie, 2013), is as follows:

$$w_1 = \frac{C_1 D^3 \left(V * \left(a * \left(\sin\left(\frac{\alpha}{2}\right) \right)^{\frac{1}{3}} \right)^b \right)^3}{H_v^{\frac{3}{2}}} \rho_p^{\frac{3}{2}} \quad \text{-----(6)}$$

Where,

w_1 = Erosion wear rate (m³/g)

C_1 = Constant

D^3 = Particles diameter (m)

V = Velocity of impact (m/s)

a = Empirical constant called the shifting coefficient

b = Empirical constant called the shifting exponent

α = Impact angles (degree)

ρ_p = Density of the particles (kg/m³)

H_v = Target material hardness (Vickers) (Pa)

1.8 Assumptions/choice of model adoption

Considering the prevalent erosion wear mechanisms in real life scenario as observed in most of the literature reviewed, the assumption that changing the impingement angles in any case, could most possibly have an impact on the normal and tangential components of the particle impact velocity on the target material (Sundararajan and Roy, 1997). Therefore, the variation of the particles impact angle and the velocity is critically taking into consideration in the analytical modelling for the present research.

This model has been used to predict erosion rate of alloys in conjunction with the experimental data in the past as reviewed in the literature reviewed. The choice of this model is due to the fact that the target materials used for the experiment are similar to the ones implored for the present study. Also, the model contains up to five parameters such as the impact angle, particle size and Vickers hardness of the material, etc., which are

amongst some of the critical parameters used in predicting erosion wear mechanism, give credence/suitability to selecting this model for the present research.

Finally, the Cambridge engineering computer software (CES) selector has been used to select the materials so as to evaluate both the cost, mechanical and physical properties of the material needed, as a preferred material for the design and manufacturing of the selected afore mentioned components.

1.9 Analysis of Results, and Findings

Firstly, (Table7) shows the chemical composition of the five alloys selected. Alloy-A and alloy-B are regarded as brittle alloys as they contain more carbon (1.4wt %) each and alloy-C, alloy-D, and alloy-E are ductile alloys with carbon content of (0.15wt %).

Table 7: Shows the chemical compositions of the five stellite alloys with (wt. %, Cobalt in balance)

| Element Specime | Co | Cr | Mo | C | Fe | Ni | Si | Mn | W | Others |
|--------------------|-------|------|-----|------|------|----|-----|-----|-----|-----------------------|
| Alloy A | 50 | 32 | 1.5 | 1.4 | 3 | 3 | 2 | 2 | 5.5 | - |
| Alloy B | 49.60 | 32 | 1.5 | 1.4 | 3 | 3 | 2 | 2 | 5.5 | - |
| Alloy C | 27.02 | 21.5 | 8 | 0.15 | 21.5 | 18 | 1.2 | 2.5 | - | 0.1Be, 0.015P, 0.015S |
| Alloy D | 58.85 | 30 | 7 | 0.15 | 0.75 | 1 | 1 | 1 | - | 0.25N |
| Alloy E | 26.65 | 22 | 8 | 0.15 | 21.5 | 18 | 1.2 | 2.5 | - | 0.1Be, 0.015P, 0.015S |

Secondly, (Table8), shows the results for the predicted Erosion Wear Rate ER (W_1), of the five different stellite alloys, with erodent particle diameter of (50 μ m), particles density of (3890kg/m³), an average coefficient value of (a = 3.4), an average exponent value of (b = -0.4), and a constant ($C_1 = 1 \times 10^6$) obtained from the adopted (Nsoesie, 2013) experimental data and the model equation as stated above, which is used in calculating the erosion wear rate of the five alloys, and with the alloys Vickers hardness (HV)(GPa).

Using alloy-A, for example, the Vickers Hardness number is given as ($H_v = 4.021 \times 10^9$ (GPa)), particles impingement angle of ($\alpha = 45^\circ, 60^\circ, \text{ and } 90^\circ$), erodent particles diameter of ($D = 50 \times 10^{-6}$ m), constant ($C_1 = 1 \times 10^6$), particles density ($\rho = 3890$ kg/m³), and particle impact velocity at ($V = 84$ m/s) respectively, inputting this values into the adopted model equation, one can predict the erosion wear rate ER (W_1), of the five stellite alloy-A, at the three different impingement angles shown above to be (1.92×10^{-11} m³/g), (1.39×10^{-11} m³/g), and (9.19×10^{-11} m³/g) obtained in that respective order as can be seen in (Table 7) below.

Table 8: Shows values of the constants (a, b, and C_1) and the predicted erosion wear rates ER (W_1), from the adopted Model

| @ Particle impact velocity of 84m/s | | | | | | | | | |
|-------------------------------------|------------------------------|--|---------------------------|-----------------|--------------|--------------------|--|--|--|
| Alloys | Particle diameter (μ m) | Particles Density (kg/m ³) | Vickers hardness HV (GPa) | Coefficient (a) | Exponent (b) | Constant (C_1) | Predicted Erosion Rate ER(w_1) (m ³ /g) $\times 10^{-11}$ for 45 ^o | Predicted Erosion Rate ER(w_1) (m ³ /g) $\times 10^{-11}$ for 60 ^o | Predicted Erosion Rate ER(w_1) (m ³ /g) $\times 10^{-11}$ for 90 ^o |
| Alloy A | 50 | 3890 | 4.021 | 3.4 | -0.4 | 1×10^6 | 1.92 | 1.39 | 9.19 |
| Alloy B | 50 | 3890 | 4.707 | 3.4 | -0.4 | 1×10^6 | 1.52 | 1.10 | 7.26 |
| Alloy C | 50 | 3890 | 7.169 | 3.4 | -0.4 | 1×10^6 | 1.08 | 5.86 | 3.86 |
| Alloy D | 50 | 3890 | 3.295 | 3.4 | -0.4 | 1×10^6 | 2.59 | 1.88 | 1.24 |
| Alloy E | 50 | 3890 | 5.394 | 3.4 | -0.4 | 1×10^6 | 1.24 | 8.97 | 5.92 |

| @ Particle impact velocity of 98 m/s | | | | | | | | | |
|---------------------------------------|----|------|-------|-----|------|-----------------|------|------|------|
| Alloy A | 50 | 3890 | 4.021 | 3.4 | -0.4 | 1×10^6 | 3.05 | 2.21 | 1.46 |
| Alloy B | 50 | 3890 | 4.707 | 3.4 | -0.4 | 1×10^6 | 2.41 | 1.75 | 1.15 |
| Alloy C | 50 | 3890 | 7.169 | 3.4 | -0.4 | 1×10^6 | 1.28 | 9.29 | 6.13 |
| Alloy D | 50 | 3890 | 3.295 | 3.4 | -0.4 | 1×10^6 | 4.11 | 2.98 | 1.97 |
| Alloy E | 50 | | 5.394 | 3.4 | -0.4 | 1×10^6 | 1.96 | 1.42 | 9.39 |
| @ Particle impact velocity of 120 m/s | | | | | | | | | |
| Alloy A | 50 | 3890 | 4.021 | 3.4 | -0.4 | 1×10^6 | 5.6 | 4.06 | 2.68 |
| Alloy B | 50 | 3890 | 4.707 | 3.4 | -0.4 | 1×10^6 | 4.42 | 3.21 | 2.12 |
| Alloy C | 50 | 3890 | 7.169 | 3.4 | -0.4 | 1×10^6 | 2.35 | 1.71 | 1.13 |
| Alloy D | 50 | 3890 | 3.295 | 3.4 | -0.4 | 1×10^6 | 7.55 | 5.48 | 3.61 |
| Alloy E | 50 | 3890 | 5.394 | 3.4 | -0.4 | 1×10^6 | 3.61 | 2.62 | 1.73 |

1.10 Erosion wear rate (w_1) analysis, evaluation/comparison

For better understanding, the evaluation of erosion wear rates of the alloys used for the three impact angles and velocity as illustrated in (Figure 4.1), it can be clearly seen that 90° impact angles recorded the highest erosion wear rate for (alloy-A, and alloy-B), 60° impact angles recorded highest in (alloy-E), 60° and

90° impingement angles are almost the same in (alloy-C, 60°), and (alloy-E, 90°), in that respective order, at the 84m/s particles impact velocity. Alloy-D appears to be the least affected by the impact angles variation at 84m/s particle impact velocity compared to the other alloys at impact angle 45° been the minimum.

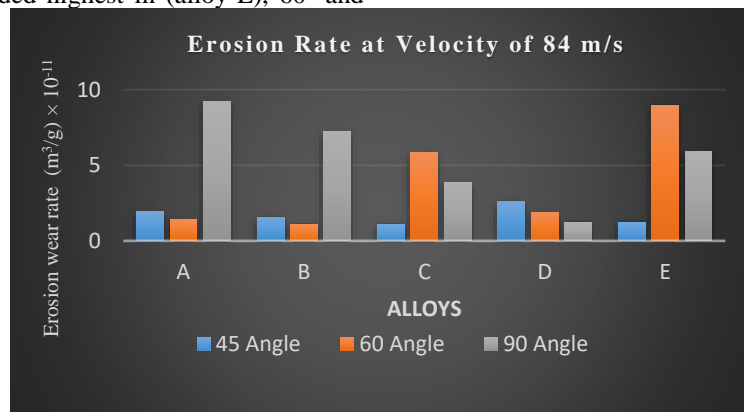


Figure 4.1: Model predicted Erosion Wear Rate of the five stellite alloys at impact velocity of (84m/s) and impingement angles of (45° , 60° , and 90° respectively)

In (Figure 4.2), the erosion wear rate for all the five alloys takes a similar form but different level of erosion wear. Alloy-D erosion wear rate is $4.11 \times 10^{-11}(\text{m}^3/\text{g})$, alloy-A erosion wear rate is slightly above $3.05 \times 10^{-11}(\text{m}^3/\text{g})$, followed by alloy-B with $2.41 \times 10^{-11}(\text{m}^3/\text{g})$, alloy-E with $1.96 \times 10^{-11}(\text{m}^3/\text{g})$, and alloy-C, which has the least erosion wear rate of $1.28 \times 10^{-11}(\text{m}^3/\text{g})$.

Also, worthy of note, is the influence of the three different angles which appears to be the same in all the alloys. This shows that at the velocity of 98m/s, the erosion wear mechanism of the five stellite alloys for the present research are not individually affected by the impingement angle. Although, they both have different levels of erosion wear rate, the various impact angles in each alloy are the same.

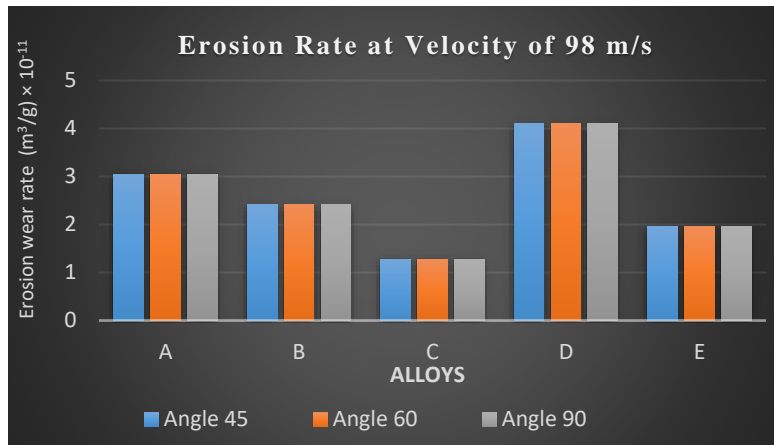


Figure 4.2: Model predicted Erosion Wear Rate of the five stellite alloys at impact velocity of (98m/s) and impingement angles of (45°, 60°, and 90°)

Alloy-D, and alloy-A, appears to be most affected at impact angle of 90° at the 120m/s velocity, with erosion wear rate of $(7.55 \times 10^{-11} \text{m}^3/\text{g})$, and $(5.60 \times 10^{-11} \text{m}^3/\text{g})$, in that respective order as illustrated in (Figure 4.3) below. Alloy-C appears to be the least affected

with erosion rate of approximately $(1.28 \times 10^{-11} \text{m}^3/\text{g})$, at impact angles of 60°, and 90° respectively.

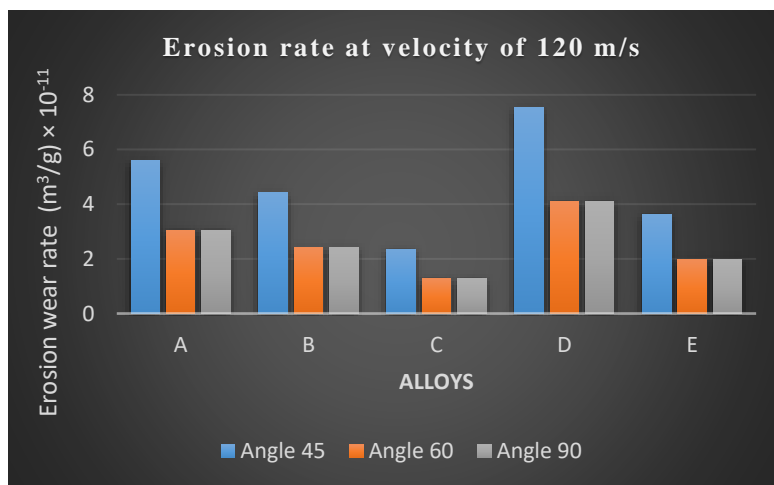


Figure 4.3: Model predicted Erosion Wear Rate of the five Stellite alloys at impact velocity of (120m/s) and impingement angles of (45°, 60°, and 90°) respectively.

All the five alloys used in the model equation, the influence of the impact angle as a key parameter with respect to erosion wear rate in oil and gas components is clearly exhibited in both the (brittle, alloy-A, and alloy-B), and (ductile alloys, alloy-C, alloy-D, and alloy-E).

Furthermore, comparison of the five alloys erosion wear rate in the three dissimilar particle impingement velocities, for instance being illustrated in all the (Figure 4.1 – 4.3) respectively, it is obvious that the erosion wear rate is much greater as the velocity of impact is increased. This gives rise to increased rate of erosion wear in all the five stellite alloys used in the model prediction at the three impact angles considered.

This is in agreement with other researchers (Nsoesie, 2013) and (Parsi et al, 2014) both experimental and analytical model results as observed in the cases studied.

The effect of the velocity parameter on erosion wear rate is observed to be least substantial mostly in the more ductile alloy-C, and alloy-D, and slightly in alloy-E, particularly at impact angle of 90°, at 84m/s, and both angles of 45°, 60°, and 90° at 98m/s, and impact angles of 90°, 60°, and 45° at 120m/s, are scarcely influenced by particle impact velocities.

1.11 Graphical analysis/presentation of the erosion wear rate predicted

To further analysis the erosion wear rate mechanism, the model predicted results are graphically presented as shown in (Figure 4.4 – Figure 4.6) below; this time from a minimum angle of 10^0 to the maximum angle of 90^0 for the different particles impingement

velocity ranging between (84m/s, 98m/s and 120m/s) respectively.

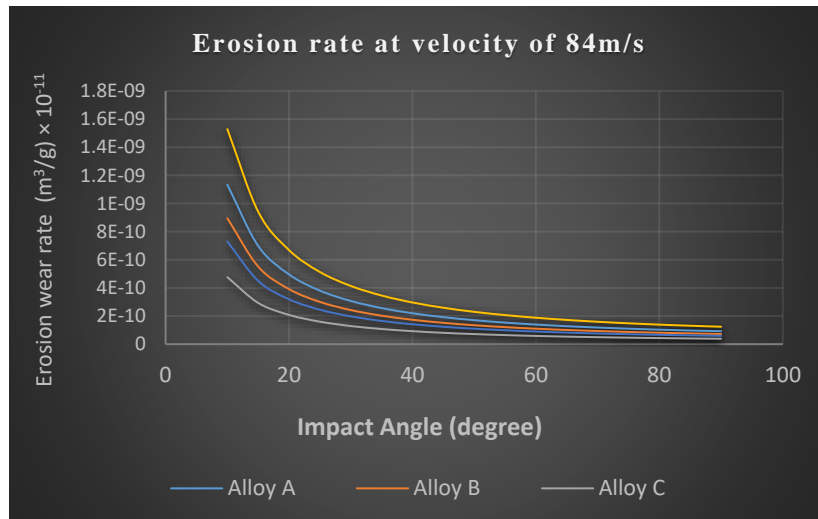


Figure 4.4: Graphical representation of the Erosion Wear Rate vs particle impact velocity of (84m/s) at impact angles of ($10^0 - 90^0$)

As can be seen in the above graph (Figure 4.4), the erosion wear rate of all the five Stellite alloys reduced with increasing impact angles at the erodent impingement velocity of 84m/s. However, this steady reduction of erosion wear rate is observed to stable at impact angle of 60^0 up to the maximum angle of 90^0 .

Furthermore, erosion wear rate at velocity 98m/s also, follows similar ductile behaviour as can be seen in the graph (Figure4.5) below; but this time standing at 65^0 and all the five alloys forming a ductile erosion wear behaviour.

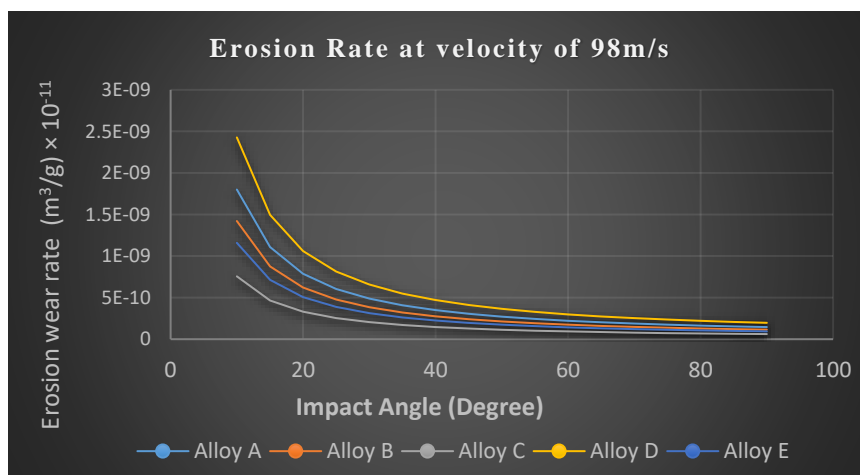


Figure 4.5: Graphical representation of the Erosion Wear Rate vs particle impact velocity of (98m/s) at impact angles of ($10^0 - 90^0$)

The same scenarios of steady decrease of erosion wear rate with increasing impact angle is observed at the erosion wear velocity of 120m/s as illustrated in the graph of (Figure 4.6) below, and attaining a steady

linear state from angle 59^0 in the linear reduction. However, agreeing to the empirical models of earlier researchers as discussed in the literature such as (Nsoesie et al, 2013) and (Kamran et al, 2011).

However, it is unclear why the erosion wear rate of the slightly brittle alloys (alloy-A and alloy-B) also follows the linear erosion wear reduction with

increasing angles, even before the critical angle of 30° generally agreed by previous researchers as the “critical angle.”

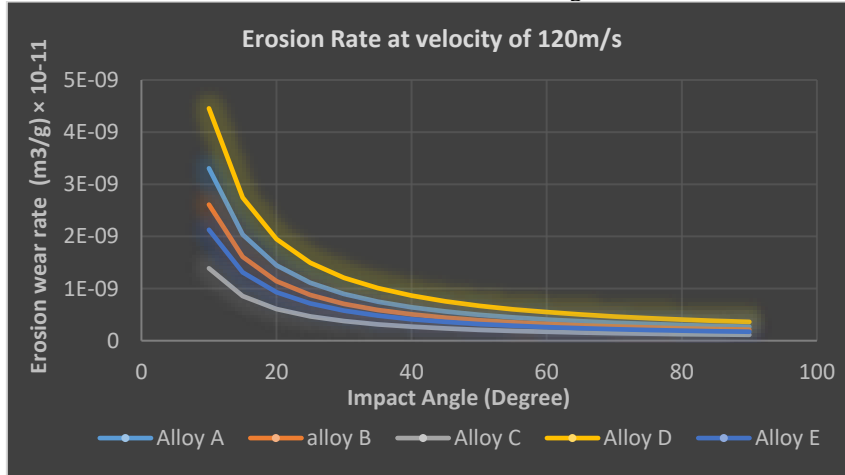


Figure 4.6: Graphical representation of the Erosion Wear Rate vs particle impact velocity of (120m/s), at impact angles of ($10^{\circ} - 90^{\circ}$) respectively.

This may not be unconnected to the fact that the carbon content in these alloys is too low which makes them to be more ductile in nature or it is a deficiency of the adopted model for predicting the erosion behaviour of these alloys. Another possible reason could be to the fact that the erosion wear rate of several materials changes significantly and that change is controlled by the shape and sizes of erodent particles as noted in the literature (Cousens et al, 1983). Therefore, the particle diameter ($50\mu\text{m}$) used for the model could be a contributing factor. It is also, generally believed amongst researchers that erosion wear rate increases with increase in the erodent particle velocity. The greater the velocity of the impingement particles, the greater the rate of erosion wear. But in the case of the present stellite alloys studied, this phenomenon is observed to be erratic in all the five

alloys and does not increase linearly with increasing velocity.

Analysis and Graphical Evaluations of the CES Stellite Alloy Materials Properties

Based on the erosion wear degradation critically evaluated in the literature reviewed and the case studies with regard to the erosion wear rate of the case study component (choke valves and separator), the selected Stellite alloys design mechanical/physical properties are evaluated using Cambridge Engineering Software (CES), and the result are graphically presented below.

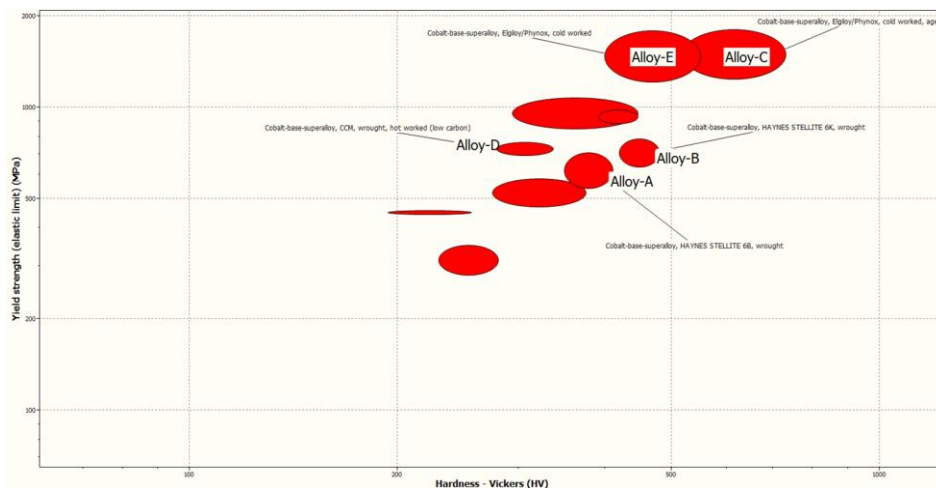


Figure 4.7: Yield strength-elastic limit vs Vickers Hardness

The first chart shown above (Figure 4.7), is the yield strength-elastic limit compared with the Vickers hardness*/tensile strength of the five Stellite alloys. The graph shows that Stellite alloys have good yield strength-elastic limit, which makes them suitable for design of oil and gas equipment critical components. Moreover, they have excellent erosion and corrosion resistance ratio as can be seen in their chemical

composition. These are important properties required considering the operating environment of the choke valves and separator which can be cavitation-erosion in the case of choke valves and erosion-corrosion due to the presence of H₂S in the separators including sand erosion in both components.

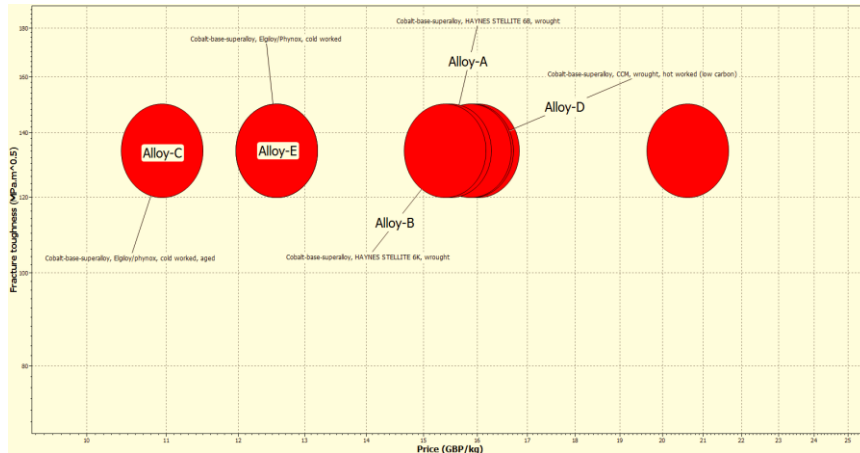


Figure 4.8: Fracture Toughness vs Price of Stellite Alloys

The next bubble chart (Figure 4.8) above, shows the comparison between fracture toughness and the price of the selected Stellite alloys. When materials with high quality of fracture toughness is required for the design of the aforementioned component, it is also imperative to consider the cost effectiveness of that material. Hence, it is so important that erosion wear resistance materials are less expensive considering the fact that after manufacturing and fabrication works are complete, the component/material could be purchased at reasonable cost price even though the oil and gas industry is adjudged to be capital intensive. In the case

studies/literatures reviewed, most researchers are observed to ignore the need for balancing the materials solutions for the manufacturing of oil and gas critical components as regard to price when dealing with erosion wear reduction.

The Stellite alloys considered as can be seen in the graph above are considerably economical which are beneficial in the manufacturing of the above-mentioned component and also, are very good in erosion wear and corrosion resistance with high strength that is suitable for oil and gas engineering applications.

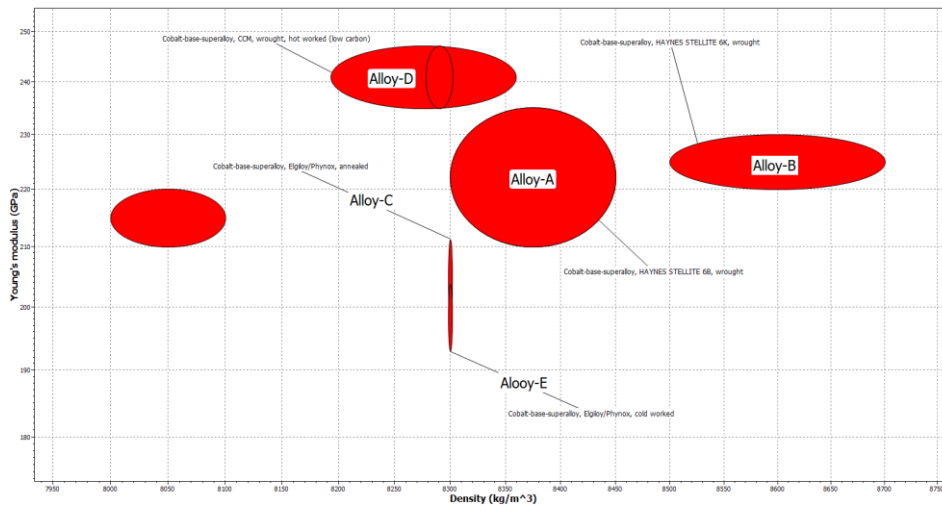


Figure 4.9: Young Modulus vs Density of Stellite Alloy Material

The final bubble chart shown above (Figure 4.9), is the chart of “Young Modulus versus the Density of the Stellite alloy materials. The core motive here is that, it is a common understanding in material selection that good Young Modulus of a material means the material is strong enough for oil and gas application. This can be seen in the graph above that, the Stellite alloys do not only have high density but also good Young Modulus ranging from (210 – 235GPa).

Also, these alloys have excellent galling and adhesive erosion wear resistance which are very advantageous properties considering the fact that the components in question will undergo such critical conditions as erosive sand particles and corrosive hydrocarbon fluids will be flowing in and through these components in their in-service condition.

V. MATERIAL SURFACE ENGINEERING/TREATMENT METHODS FOR STELLITE ALLOYS WEAR REDUCTION MECHANISM.

There are many surface engineering and treatment methods that can be applied in treating materials for engineering (oil and gas) application as illustrated in (Figure 5.1) below.

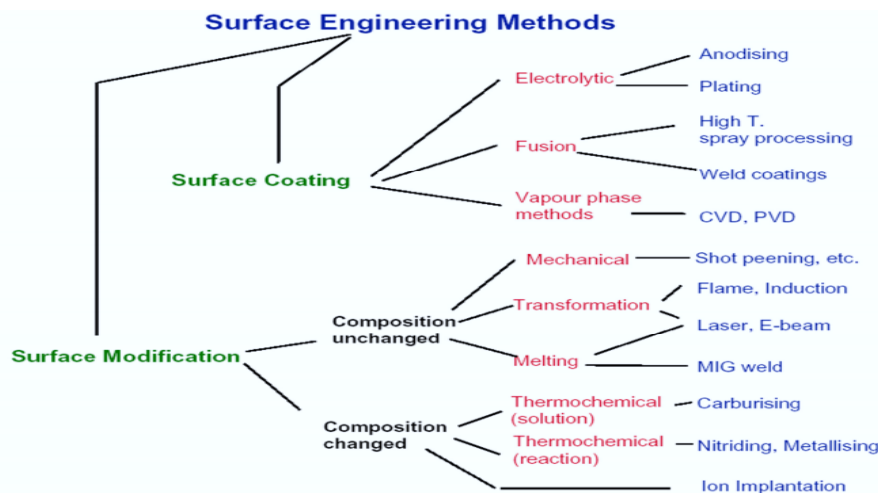


Figure 5.1: material Surface Engineering/treatment methods (Ashby and Cebon, 1993), and (Swanson, 2016: Lecture)

Primarily, considerations for applying any of these methods for treating a component could depend on the nature of the environment and the degree of wear resistance required in the in-service conditions of the component in operation (Swanson, 2016).

Just as every other alloy material, the plasma surface engineering alloying (PSA) method of treatments could effectively improve the erosion wear properties of Stellite alloys both in (3.5% NaCl) solution and in air as been demonstrated with (cast Stellite alloy-21), which shows that, the advanced (PSA) treated surface stiffness, the lesser the wear influence and the improved the erosion wear resistance of the alloy (Chen et al, 2008).

Surface treatment using laser cladding has excellent metallurgical bonding with slight intermixing with the bulk material and little distortions which means only slight machining could be required after deposition process is done (D’Oliverira, da Silva, and Vilar, 2002).

In all, the species are produced in the vapour phase, a coating typically (1 - 20µm) thickness is moulded (formed) on the substrate of which the vapour consisting atoms or ions of the target material as commonly in a solid or liquid state that has been removed from the target by sputtering-collisions with similar atoms or by evaporation. Techniques includes resistive heating-common for evaporation temperature below 1800°C and high energy electron beam-used for temperature above 1800°C evaporation (Mellor, 2006).

These coating processes as earlier mentioned are very complex procedures and any consideration of selecting one of this process should be done in respect of required capabilities for the components and financial consideration as most of the processes are expensive. Although modern engineering materials surface design processes are considered even before the component is manufactured which has already

considered both compatibility of the process with regards to the substrate, technical and economic, yet it should be properly evaluated (Mellor, 2006). However, material surface coating process is often used to improve the material properties if a component failure rate is intolerable (Mellor, 2006), as in the case of some choke valves trims in the North Sea.

Summarily, the following surface engineering/treatment could be possible with stellite alloys:

- Stellite alloy surface hardness could be increased by (2–3) times more using the method of plasma surface alloying with carburising and nitriding treatment process.
- The factor of sliding wear of these alloys both in air and (3.5 NaCl) solution could reduce by (99% and 96%) in that order with plasma material surface alloying treatment process.
- The ‘S-phase’ could be formed in these alloys with plasma surface alloying treatment at (400 – 460°C) as low temperature scenario. However, chromium nitride precipitation could be possible in the treated surface layers at higher temperatures, say up to (550°C) (Chen et al, 2008).]

1.12 Discussion of Results: Chemical composition and microstructural effects of stellite alloys

Materials microstructure is determined by both the chemical compositions, desired heat treatment requirement, processes for fabrication, cold and hot working processes contributes, and controls the overall mechanical and physical properties of the required products which the material is used to produce (Swanson, 2016).

The importance of carbon content in a material cannot be overemphasised, and it is a critical parameter in the carbide volume fraction of the Stellite alloys. For the alloys considered in the present research, the carbon content from alloys-C to alloy-D are less than one (0.15wt %) therefore, could be as solution strengthening alloys in all respect.

The microstructure of these alloys as observed in the literature reviewed, Stellite alloys contains very small number of carbides which is complemented by the high molybdenum intermetallic element of (Co_3Mo and CoMo_6) that decreases the ductility and increases the (hardness) in the alloy’s microstructure.

However, alloy-A and alloy-B comprises slightly higher carbon content (1.5wt %) compared to the other alloys, which forms the primary carbides (Cr_7C_3) microstructures. Also, the presences of other element such as tungsten and chromium are crucial in the microstructure of these alloys as indicated in alloy-A and B; and also discussed in (chapter three) of this research. The presences of these tungsten-cobalt-

carbon carbides in the Stellite alloys enhances the erosion wear resistance and hardness.

The indispensability of chromium in erosion wear resistance oil and gas alloys is also observed in the Stellite alloy microstructure. A substantial amount of chromium ranging from (21.5 to 32wt %), is present in all the alloys which contributes to the erosion wear resistance chromium-carbide, and corrosion-oxidation resistance required in these alloys. The face centred cubic (FCC) matrix form of stability in these alloys is provided by the presence of slightly high nickel content in all the five Stellite alloys which ranges from (1 to 18wt%) that effectively serving as machinability enhancer (Davis, 2000: p362-406) and (Opris, 2007: p.581-591).

1.13 Contrast between Erosive Wear Resistance and Microstructures of Stellite Alloys

Evidently, the erosion wear resistibility is sturdily depended or influenced by the microstructure of any material as also the case of the Stellite alloys. More so, the erosion wear resistibility of these alloys or in any oil and gas materials depends on the erosion wear conditions prevalent in the operating environment-conditions and flow parameters such as the impingement angle, particle diameter, fluid velocity and particles density. The ‘erosion wear rate of any material, stellite alloy inclusive, has an inverse proportionality relationship to the number of intermetallic compounds and carbide volume fraction present in the alloy’ (Nsoesie, 2013).

Therefore, the presence of the carbide-intermetallic compounds forms a protective film of resistance, which could impel the erosion mechanism of cutting and target materials extensive distortion activities. It is also worthy to note here that it appears Stellite alloys possess more compressive strength compared to tensile strength as observed in the erosion rate graph presented. This explains their higher erosion resistibility with increasing impact angles (90°) as can be seen in all the graphs above.

In most engineering metallic materials such as Stellite alloys, that are relatively ductile in nature in contrast with ceramics, erosion wear rate is seen to increase firstly with increasing particles impact angles through to the critical angle which is within (30°) and starts declining from that point as also, illustrated in the works of (Kamran et al, 2011). When the impingement angle is lesser say ($15^\circ - 20^\circ$), tensile-plastic strain is generated by impacting particles at the target point materials subsurface as a result of shearing actions that are alike with material sliding wear mechanism, of which repeated particle impact will cause accumulation of plastic distortion. Further accumulation of this strain causes the work hardening of the material subsurface

microstructures as the material strain limits is exceeded which could lead to surface material removal actions and erosion wear damage to the material (Swanson, 2016).

However, contrary to this phenomenon, it is observed that erodent particles normally impinge target material surface which causes distortion of material surface scab (layers) when the impingement angle is (90^0), and compressive stress-strain behaviour is generated in the surface scab (layer) of the material. Spalling off of the material surface coating will occur which will add to the erosion wear losses of the material at the maximum angle of (90^0) once the compressive straining of the surface coating reaches the limit of the material.

1.14 Vickers Hardness Effect versus Erosion Wear Resistance of Stellite Alloys

Stellite alloys and every other metallic material such as over-lays and hard-facing, cobalt base coatings, chemical nickel coatings, tungsten-carbides coatings, which includes different carbide/nickel binders' materials in engineering application with regards to erosion wear resistance are qualitatively judged by their Vickers hardness (HV) (Frenk and Wagniere, 1991: p.65-68).

Also, as observed from the case studies, majority of previous researchers agreed with the fact that the harder an engineering material, the superiority of that material in resisting wear. This point is also corroborated by the works of (Kapoor, 2011) which shows that material hardness plays a principal starring-roles in regulating the sliding wear resistibility of stellite alloys when temperature is within room temperature-conditions.

5.4 Conclusion and Recommendation for Further Works

A comprehensive investigation has been embarked upon in a bid to understanding the complex erosion wear phenomenon that is prevalent in oil and gas critical components in a view to proffering a material solution in reducing wear and erosion in the oil and gas industry. It is understood that material erosion wear in oil and gas components is mainly due to entrain/suspended solid particles flowing through and into hydrocarbon production, transportation and processing equipment's, causing severe material degradation. The most critical erosion wear mechanism is the erosion caused by solid particles (fine, sands and other reservoir impurities), flowing in the production systems (Nokleberg *et al*, 1995). Statistical analyses/evaluation of the erosion wear rate, and graphical presentation of the results

were completed, and the following conclusions are deduced from the present study:

- The predominant-critical erosion and wear mechanism of oil and gas equipment is the erosion-wear phenomenon by solid particles impingement. Therefore, to reduce the erosion rate of critical oil and gas component, the focus should be on finding a combination of developing erosion wear resistant materials/alloys and improving the operational conditions, the design geometry of the productions equipment such as choke valves, separators, pipelines and the fluid flow parameters such as velocity. The profound solution to the problematic solid particle erosion wear for instance in choke valves, is the reduction of the impingement angle and application of erosion wear resistance materials such as stellite alloys as target materials in designing the critical components mostly affected zones.
- The main parameter governing the Stellite alloys erosion wear resistibility is the carbon composition which contributes to the carbide fractional volume of the alloys and the carbon composition as a key parameter in these alloys. The strength of this alloys is provided by tungsten and molybdenum. Therefore, increase in tungsten-molybdenum compositions of these alloys will effective increase their erosive-wear performance in both erosion-corrosion prone applications.
- There were two key mechanisms observed to be involved in the Stellite alloys particles impact erosion wear damage/distortion process. These includes: Surface material 'cutting' that results in sagging lips, and surface materials 'plastic deformation' that causes the surface coatings removal.
- Experimental evidence in the case studied indicates that at impact angles of 30^0 , material damage processes are largely due to the tensile-plastic distortion of subsurface materials layers by shearing influence and at impact angle of 90^0 , concentrated compressive-stresses are mainly the causes of the materials damage mechanism due to the overburden loads at normal impingement (Nsoesie, 2013).
- Stellite alloys rate of erosion wear is observed to be high at (45^0) impact angle when compared with the (90^0) impact angle. The rate of erosion at smaller angles says ($10^0 - 20^0$) is even higher and gradually decreases when approaching the critical angle of (30^0). This trend is also observed in other materials as shown in the works of (Parsi *et al*, 2014). This behaviour could be due to the stellite alloys compressive strength being slightly high compared to that of their tensile strength.

- The transitional behaviour of alloy-A and alloy-B as the target material showing some effects from been brittle in lesser velocity to been ductile as the velocity increases needs further experimental clarifications.
- Also, as it is a common knowledge in the oil and gas industry that hydrocarbon fluids do not flow mostly as a single-phase entity. Therefore, the area of multiphase fluid flow erosion wear mechanism in oil and gas critical components with their complex geometry should be given more attention. There are reported cases of choke valves trim been eroded in just few months in the North Sea for severe sand erosion wear conditions (Haugen, 1995). This means that more experiment should be conducted to understand the multiphase erosion wear phenomenon in such critical component.
- Hydrocarbon fluid viscosity effect in the rate of erosion wear is observed to be neglected in most of the cases studied, both in the experimental results and in the models' equations. This parameter should also be considered in further experimental research to know its contribution in the erosion wear mechanism.
- Hydrocarbon liquid droplet in form of cavitation erosive-wear is also, observed to be critical issue in the complex erosion wear phenomenon. Cavitation in this context of the present research means liquid-droplets that erode majorly the valve trim, body and downstream pipe walls as earlier discussed. It is therefore, necessary to conduct erosion wear test at lesser impingement angles and substantial reduction of liquid droplet velocity and liquid implosion before striking the target material walls.
- Finally, the economical/cost-effectiveness of alloying materials in general for erosion wear reduction in the oil and gas industry application should also be given attention in future research due to the falling global oil price and this will increase the cost-effectiveness material solutions in combatting the complexity of erosion wear mechanism.
- Temperature effect on erosion rate have a complex dependency on the particle shape as the main erosion mechanism of 'erosion oxidation' been a critical function of the particle size/shape (Sundararajan and Roy, 1997). However, according to (Levy, 1995) and (Grotzbach, 1996), elevated temperature on erosion wear of (9Cr – 1Mo steel at velocity of 30m/s and temperature of 850°C), and angular (SiC) as the erodent particle obviously shows more erosion wear rate rather than (Al₂O₃), that has a round shape.
- Generally, further experiment should be conducted on erosion resistant materials at typical

oil and gas field temperatures for potential future materials in other to determine the effects of temperature on these alloys.

1.15 Limitations

There are some few limitations observed in the present research. Foremost among them is the time limitation which constrained the researcher from include some modern means of studying erosion wear rate such as finite element analysis (FEA) and computational fluid dynamics (CFD) of the flow pattern in the chosen component to determine the reliability of the material selected and the model prediction results as well. Also, the number of materials considered is restricted to Stellite alloys alone, which is not broad enough to determining the most suitable materials needed for the designing and manufacture of the selected components.

REFERENCES

- [1]. Akbarzadeh, E., Elsaadawy, E., Sherik, A.M., Spelt, J.K. and Papini, M. (2012) 'The solid particle erosion of 12 metals using magnetite erodent', *Wear*, 282-283, pp.4051. doi:10.1016/j.wear.2012.01.021.
- [2]. AlBukhaiti, M.A., AbouelKasem, A., Emar, K.M. and Ahmed, S.M. (2016) 'Particle shape and size effects on slurry erosion of AISI 5117 steels', *Journal of Tribology*, 138(2), p.024503. doi:10.1115/1.4031987.
- [3]. American Society for Testing and Materials (1968) *Analytical Chemistry*, 40(6), pp.150A-150A. doi:10.1021/ac60262a859.
- [4]. American Society for Testing and Materials. and American Society for Testing and Materials. (1978) *1978 annual book of ASTM standards: Pt.43: Electronics*. Philadelphia: The Society.
- [5]. Arabnejad, H., Mansouri, A., Shirazi, S.A. and McLaury, B.S. (2015) 'Evaluation of Solid Particle Erosion Equations and Models for Oil and Gas Industry Application', *SPE Annual Technical Conference and Exhibition*. Houston, Texas, USA, 28-30 September 2015, 2015. Houston, Texas, USA: Society of Petroleum Engineering. pp.1-21.
- [6]. Arefi, B., Setari, A. and Angman, P. (2006) 'Simulation of erosion in drilling tools for the oil and gas industry', *Journal of Canadian Petroleum Technology*, 45(11). doi: 10.2118/06-11-04.
- [7]. Ashby, M.F. and Cebon, D. (1993) 'Material selection in mechanical design', *Le Journal de Physique II*, 03(C7), pp.C7-1-C7-9. doi:10.1051/jp4:1993701.

- [8]. Ashby, M.F. and Jones, D.R.H. (2005) *Engineering materials 2: An introduction to microstructures, processing and design*. Butterworth-Heinemann. ASTM Designation, G32-03, Standard Test Method for Cavitation Erosion Using Jibrot 01y Evaluation, 032-03, pp.106-119.
- [9]. ASTM standards on copper and copper alloys. ASTM committee B-5, on copper alloys, cast and wrought, copper and copper alloys, cast and wrought, copper and copper alloy electrical conductors, non-ferrous metals used in copper alloys. 116-116. doi:10.1002/maco.19570080229.
- [10]. Atapek, S. H. and Fidan, S. (2015) 'Solid particle erosion behavior of cast alloys used in the mining industry', *International Journal of Minerals, Metallurgy, and Materials*, 22(12), pp. 1283-1292. doi: 10.1007/s12613-015-1196-6.
- [11]. Bellman, R. and Levy, A. (1981) 'Erosion mechanism in ductile metals', *Wear*, 70(1), pp. 1-27. doi:10.1016/0043-1648(81)90268-4.
- [12]. Bitter, J.G.A. (1963) 'A study of erosion phenomena', *Wear*, 6(3), pp. 169-190. doi: 10.1016/0043-1648(63)90073-5.
- [13]. Chen, J., Li, X.Y., Bell, T. and Dong, H. (2008) 'Improving the wear properties of Stellite 21 alloy by plasma surface alloying with carbon and nitrogen', *Wear*, 264(3-4), pp. 157-165. doi: 10.1016/j.wear.2006.12.012.
- [14]. Chen, J., Li, X.Y. and Dong, H. (2010) 'Formation and characterization of S phase in plasma carburised high carbon Stellite 21 CoCrAlloy', *Surface Engineering*, 26(4), pp. 233-241. doi:10.1179/026708409x12490360426007.
- [15]. Cong, D., Jian-Zhong, L., Zhen-Yu, H., Jun-Hu, Z. and Ke-Fa, C. (2010) 'VOF method for impinging-jet Atomizers', *Energy & Fuels*, 24(1), pp. 451-455. doi: 10.1021/ef900665g.
- [16]. Cousens, A.K. (1984) 'The Erosion of Ductile Metals by Solid Particle Impact (doctoral thesis)', University of Cambridge.
- [17]. Cousens, A.K. and Hutchings, J.M. (1983) 'A critical study of the erosion of an aluminium alloy by solid spherical particles at normal impingement', *Wear*, 88(3), pp. 335-348. doi:10.1016/0043-1648(83)90302-2.
- [18]. Davis, J.R. (2001) 'ASM specialty handbook: Nickel, cobalt, and their alloys', *Choice Reviews Online*, 38(11), pp. 38-6206-38-6206. doi: 10.5860/choice.38-6206.
- [19]. Desale, G.R., Gandhi, B.K. and Jain, S.C. (2009) 'Particle size effects on the slurry erosion of aluminium alloy (AA 6063)', *Wear*, 266(11-12), pp. 1066-1071. doi: 10.1016/j.wear.2009.01.002.
- [20]. D'Oliveira, A.S.C.M., da Silva, P.S.C.P. and Vilar, R.M.C. (2002) 'Microstructural features of consecutive layers of Stellite 6 deposited by laser cladding', *Surface and Coatings Technology*, 153(2-3), pp. 203-209. doi: 10.1016/S0257-8972(01)01687-5.
- [21]. Engineering, P. (2014) 'Oil processing on offshore facilities'. Available at: Total SA: Total worldwide (2006). Available at: <http://www.totalproductionandexploration.com> (Accessed: 12 August 2016). accessed from Total worldwide website
- [22]. Finnie, I. (1960) 'Erosion of surfaces by solid particles', *Wear*, 3(2), pp. 87-103. doi: 10.1016/0043-1648(60)90055-7.
- [23]. Grotzbach, M. (1996) 'Solid particle erosion and erosion-corrosion of materials'. Von Alan V. Levy, 220 Seiten, ASM International, materials park. Ohio 1995, £84.00, ISBN 0-87170-519-2, Materials and Corrosion/Werkstoff und Korrosion, 47(12), pp. 715-715. doi:10.1002/maco.19960471211.
- [24]. Hattori, S. and Mikami, N. (2009) 'Cavitation erosion resistance of stellite alloy weld overlays', *Wear*, 267(11), pp. 1954-1960. doi: 10.1016/j.wear.2009.05.007.
- [25]. Haugen, K., Kvernemo, O., Ronold, A. and Sandberg, R. (1995) 'Sand erosion of wear-resistant materials: Erosion in choke valves', *Wear*, 186-187, pp. 179-188. doi: 10.1016/0043-1648(95)07158-x.
- [26]. Heathcock, C.J., Ball, A. and Protheroe, B.E. (1981) 'Cavitation erosion of cobalt-based Stellite alloys, cemented carbides and surface-treated low alloy steels', *Wear*, 74(1), pp. 11-26. doi: 10.1016/0043-1648(81)90191-5.
- [27]. Henni, A. (2013a) 'Saudi Aramco expands reach through new technology centers', *Journal of Petroleum Technology*, 65(08), pp. 74-77. doi: 10.2118/0813-0074-jpt.

- [29]. Henni, A. (2013b) 'Saudi Aramco oil and gas production hit historic levels', *Journal of Petroleum Technology*, 65(09), pp. 86-87. doi: 10.2118/0913-0086-jpt.
- [30]. Hutchings, I. M. (1981) 'A model for the erosion of metals by spherical particles at normal incidence', *Wear*, 70(3), pp. 269-281. doi: 10.1016/0043-1648(81)90347-1.
- [31]. Hutchings, I. M. and Winter, R. E. (1974) 'Particle erosion of ductile metals: A mechanism of material removal', *Wear*, 27(1), pp. 121-128. doi: 10.1016/0043-1648(74)90091-x.
- [32]. Ives, L. K. (1977) 'Erosion of 310 stainless steels at 975°C in combustion gas atmospheres', *Journal of Engineering Materials and Technology*, 99(2), p. 126. doi: 10.1115/1.3443421.
- [33]. Jones, D. R. H. and Ashby, M. (2005) *Engineering materials I: An introduction to properties, applications and design*. United Kingdom: Butterworth-Heinemann.
- [34]. Kim, Y.-B., Lee, K. and Chung, J.-H. (2002) 'Optimum cleaning-in-place conditions for stainless steel microfiltration membrane fouled by terephthalic acid solids', *Journal of Membrane Science*, 209(1), pp. 233-240. doi: 10.1016/S0376-7388(02)00347-2.
- [35]. Kleis, L. R. (2008) *Solid particle erosion: Occurrence, prediction and control*. United States: Springer Verlag London.
- [36]. Kraus, M. and Krewer, U. (2011) 'Experimental analysis of the separation efficiency of an orientation independent gas/liquid membrane separator', *Separation and Purification Technology*, 81(3), pp. 347-356. doi: 10.1016/j.seppur.2011.08.001.
- [37]. Laguna-Camacho, J. R., Martinez-Garcia, H., Escamilla-Rodriguez, F., Alarcon-Rosas, C., Calderón-Ramón, C. M., Rios-Velasco, L., Pelcastre-Lozano, M., Casados-Sanchez, A. and Gonzalez-Gomez, M. (2015) 'Erosion behavior of AISI 6061-T6', *Journal of Surface Engineered Materials and Advanced Technology*, 05(03), pp. 136-146. doi: 10.4236/jsemat.2015.53015.
- [38]. Levy, A. V. (1995) 'Erosion and erosion-corrosion of metals', *Corrosion*, 51(11), pp. 872-883. doi: 10.5006/1.3293564.
- [39]. Levy, Alan V. (1995) *Solid particle erosion and erosion-corrosion of materials*. United States: ASM International.
- [40]. Levy, D., Abraham, R. and Reid, G. (1991) 'MATTERS ARISING: Levy et al reply', *Journal of Neurology, Neurosurgery & Psychiatry*, 54(2), pp. 188-188. doi: 10.1136/jnnp.54.2.188.
- [41]. McCabe, L. P., A. Sargent, G. and Conrad, H. (1985a) 'Effect of microstructure on the erosion of steel by solid particles', *Wear*, 105(3), pp. 257-277. doi: 10.1016/0043-1648(85)90072-9.
- [42]. McCabe, L. P., A. Sargent, G. and Conrad, H. (1985b) 'Effect of microstructure on the erosion of steel by solid particles', *Wear*, 105(3), pp. 257-277. doi: 10.1016/0043-1648(85)90072-9.
- [43]. Mellor, B. G. (ed.) (2006) *Surface coatings for protection against wear*. United Kingdom: Woodhead Publishing.
- [44]. Misra, A. and Finnie, I. (1981) 'On the size effect in abrasive and erosive wear', *Wear*, 65(3), pp. 359-373. doi: 10.1016/0043-1648(81)90062-4.
- [45]. Mulyandasari, V. and Kolmetz, K. (2011) *KLM technology group practical engineering guidelines for processing plan/solutions separator vessel selection and sizing (engineering design guideline)*. Available at: http://kolmetz.com/pdf/edg/engineering_design_guideline_separator%20vessel_REVOI.pdf (Accessed: 13 August 2016).
- [46]. Neilson, J. H. and Gilchrist, A. (1968) 'Erosion by stream of solid particles', *Wear*, 11(2), pp. 111-122. doi: 10.1016/0043-1648(68)90591-7.
- [47]. Ninham, A. (1988) 'The effect of mechanical properties on erosion', *Wear*, 121(3), pp. 307-324. doi: 10.1016/0043-1648(88)90208-6.
- [48]. Nøkleberg, L. and Søntvedt, T. (1995) 'Erosion in choke valves - oil and gas industry applications', *Wear*, 186-187, pp. 401-412. doi: 10.1016/0043-1648(95)07138-5.
- [49]. Nøkleberg, L. and Søntvedt, T. (1998) 'Erosion of foil & gas industry choke valves using computational fluid dynamics and experiment', *International Journal of Heat and Fluid Flow*, 19(6), pp. 636-643. doi: 10.1016/S0142-727X(98)10039-5.
- [50]. Oka, Y. I., Mihara, S. and Yoshida, T. (2009) 'Impact-angle dependence and estimation of erosion on a ceramic material caused by solid particle impact', *Wear*, 267(1-4), pp. 129-135. doi: 10.1016/j.wear.2008.12.091.
- [51]. Oka, Y. I., Ohnogi, H., Hosokawa, T. and Matsumura, M. (1997) 'The impact angle dependence of erosion damage caused by solid particle impact', *Wear*, 203-204, pp. 573-579. doi: 10.1016/S0043-1648(96)07430-3.
- [52]. Oka, Y. I., Okamura, K. and Yoshida, T. (2005) 'Practical estimation of erosion damage caused by solid particle impact', *Wear*, 259(1-6), pp. 95-101. doi: 10.1016/j.wear.2005.01.039.
- [53]. Oka, Y. I. and Yoshida, T. (2005) 'Practical estimation of erosion damage caused by solid particle impact'

- mpact', *Wear*, 259(1-6), pp. 102-109. doi: 10.1016/j.wear.2005.01.040.
- [54]. Parsi, M., Najmi, K., Najafifard, F., Hassani, S., McLaury, B.S. and Shirazi, S.A. (2014) 'A comprehensive review of solid particle erosion modeling for oil and gas wells and pipelines applications', *Journal of Natural Gas Science and Engineering*, 21, pp. 850-873. doi: 10.1016/j.jngse.2014.10.001.
- [55]. Prasad, P., Guru, G.S., Shivakumar, H.R. and Sheshappa Rai, K. (2012) 'Investigation on Miscibility of sodium Alginate/Pullulan blends', *Journal of Polymers and the Environment*, 20(3), pp. 887-893. doi: 10.1007/s10924-012-0427-4.
- [56]. Qin, F., Hu, J., Chou, Y.K. and Thompson, R.G. (2009) 'Delamination wear of nano-diamond coated cutting tools in composite machining', *Wear*, 267(5-8), pp. 991-995. doi: 10.1016/j.wear.2008.12.065.
- [57]. Raask, E. (1969) 'Tube erosion by ash impaction', *Wear*, 13(4-5), pp. 301-315. doi: 10.1016/0043-1648(69)90252-x.
- [58]. Raask, E. (1982) 'Flame imprinted characteristic of ash relevant to boiler slagging, corrosion, and erosion', *Journal of Engineering for Power*, 104(4), p. 858. doi: 10.1115/1.3227356.
- [59]. Roth, J. (2001) 'Shock waves in quasicrystals', *Ferroelectrics*, 250(1), pp. 365-368. doi: 10.1080/0015019008225102.
- [60]. Scheffler, M. and Colombo, P. (eds.) (2006) *Cellular ceramics: Structure, manufacturing, properties and applications*. Germany: Wiley-VCH Verlag GmbH. Solid particle erosion and corrosion of materials (1996) *Choice Reviews Online*, 33(05), pp. 33-2760-33-2760. doi: 10.5860/choice.33-2760.
- [61]. Sundararajan, G. and Roy, M. (1997) 'Solid particle erosion behavior of metallic materials at room and elevated temperatures', *Tribology International*, 30(5), pp. 339-359. doi: 10.1016/S0301-679X(96)00064-3.
- [62]. Swanson, D.P. (2016) *M04MAM: Engineering Materials for Oil & Gas - Lecture Notes and Face-faced discussions to John Bull T. T. 1st Tor*, 20 April. Lecture Notes
- [63]. Tilly, G.P. (1969) 'Erosion caused by airborne particles', *Wear*, 14(1), pp. 63-79. doi: 10.1016/0043-1648(69)90035-0.
- [64]. Tilly, G.P. (1973a) 'A two-stage mechanism of ductile erosion', *Wear*, 23(1), pp. 87-96. doi: 10.1016/0043-1648(73)90044-6.
- [65]. Tilly, G.P. and Sage, W. (1970) 'The interaction of particle and material behavior in erosion processes', *Wear*, 16(6), pp. 447-465. doi: 10.1016/0043-1648(70)90171-7.
- [66]. Wang, D.F. and Mao, Z.Y. (1996) 'A study of erosion of Si₃N₄ ceramics by impact of solid particles', *Wear*, 199(2), pp. 283-286. doi: 10.1016/0043-1648(95)06850-3.
- [67]. Yao, J., Zhou, F., Zhao, Y., Yin, H., Guo, Q. and Li, N. (2015) 'Experimental investigation of erosion of stainless steel by liquid-solid flow jet impingement', *Procedia Engineering*, 102, pp. 1083-1091. doi: 10.1016/j.proeng.2015.01.231.